JOURNAL OF PETROLOGY | VOLUME 53 | NUMBER 9 | PAGES 1867–1886 | 2012 | doi:10.1093/petrology/egs036

Petrogenesis of High-MgO Lavas of the Lower Mull Plateau Group, Scotland: Insights from Melt Inclusions

DAVID W. PEATE[1]*, INGRID UKSTINS PEATE[1], MICHAEL C. ROWE[1,2], JAY M. THOMPSON[1,3] AND ANDREW C. KERR[4]

[1]DEPARTMENT OF GEOSCIENCE, UNIVERSITY OF IOWA, 121 TROWBRIDGE HALL, IOWA CITY, IA 52242, USA

[2]SCHOOL OF EARTH AND ENVIRONMENTAL SCIENCES, WASHINGTON STATE UNIVERSITY, PULLMAN, WA 99164-1812, USA

[3]ARC CENTRE OF EXCELLENCE IN ORE DEPOSITS, UNIVERSITY OF TASMANIA, HOBART, TASMANIA 7001, AUSTRALIA

[4]SCHOOL OF EARTH AND OCEAN SCIENCES, CARDIFF UNIVERSITY, PARK PLACE, CARDIFF CF10 3YE, UK

RECEIVED MAY 27, 2011; ACCEPTED MAY 4, 2012
ADVANCE ACCESS PUBLICATION JUNE 20, 2012

Published data on Palaeogene flood basalts of the lower Mull Plateau Group (Scotland) show that the most primitive lavas (MgO > 8 wt %) have the greatest extent of crustal assimilation, inconsistent with a simple coupled assimilation–fractional crystallization (AFC) model. We present elemental data on rehomogenized olivine-hosted melt inclusions from four high-MgO flows to investigate the nature of crustal assimilation and melt aggregation processes during the initial stages of flood basalt magmatism on Mull. Whole-rock compositions have been variably modified by hydrothermal alteration associated with the nearby Central Complexes. Nd isotope compositions, which should be insensitive to this alteration, are lower than typical mantle values (ε_{Nd} + 2·4 to −5·7), indicating variable modification by crustal assimilation in all four samples. Melt inclusions are protected against alteration effects within their host olivine crystals, and provide more robust estimates of magmatic liquid compositions than whole-rocks, particularly for the alkali elements Na, K and Ba. The whole-rock samples show limited variations in Na_2O (2·4–2·8 wt %) and K_2O (0·23–0·29 wt %), despite a wide range in immobile elements (e.g. Zr 62–126 ppm). In contrast, the melt inclusions show far greater variability in Na_2O (1·8–4·0 wt %) and K_2O (0·02–0·35 wt %) and positive correlations between K and Na. Melt inclusions from different samples show systematic correlations between alkalis (K + Na) and incompatible element ratios (e.g. Zr/Y), indicating that the inclusions record magmatic values for the fluid-mobile elements. For the two most incompatible-element-enriched samples, the whole-rock analyses are similar to the melt inclusions except for lower Na and higher Ba that are related to alteration. Therefore, the crustal assimilation in these magmas must have taken place prior to growth of the olivines. For the two more depleted samples, the inclusions have less contaminated compositions than the whole-rocks, and show broad trends of increasing K/Ti with decreasing Fo% of the host olivine. For these samples, crustal assimilation must have taken place both during and after growth of the olivines and in an AFC style in which assimilation is linked to magmatic differentiation. Melt inclusions from single samples show limited variability in Zr/Y compared with K/Ti, indicating that aggregation of melts from different parts of the melt column must have occurred at deeper levels prior to growth of the olivines in the samples. Although the whole-rock compositional variations capture the broad details of crustal assimilation and melting histories for the Mull lavas despite the variable effects of hydrothermal alteration, the melt inclusion data more clearly resolve significant details of these magmatic processes. The extent of assimilation and differentiation is linked to the depth of magma stalling: primitive, contaminated magmas in the lower crust vs. evolved, uncontaminated magmas at sub-Moho depths.

KEY WORDS: *olivine; melt inclusion; Mull; flood basalts; crustal assimilation; alteration*

*Corresponding author. Telephone: (319) 354 0567. Fax: (319) 354 1821. E-mail: david-peate@uiowa.edu

INTRODUCTION

During the formation of continental flood basalt provinces large volumes of mafic magma are transported through the continental crust and stored at different crustal levels prior to eruption. Modification of mantle-derived magma compositions through interaction with crustal material is an expected consequence of such crustal transport and storage, and there is extensive evidence from many provinces for varying and significant extents of crustal assimilation (e.g. Brandon *et al.*, 1993; Kerr *et al.*, 1995; Baker *et al.*, 1996; Peate & Hawkesworth, 1996; Peate *et al.*, 2003, 2008). The style and depth of crustal assimilation will change with the progressive development of a flood basalt province in response to changes in melt supply rates and from tectonically driven modifications to the magmatic plumbing systems (e.g. Andreasen *et al.*, 2004; Fowler *et al.*, 2004; Peate *et al.*, 2008). Cooling of magmas within the crust leads to extensive crystallization, and the released latent heat provides an important heat source for melting the crustal wall-rocks (e.g. Bowen, 1928). Hence, there is a general expectation that the extent of assimilation should be linked to an index of differentiation (e.g. DePaolo, 1981), although more rigorous treatment of energy conservation during linked assimilation and crystallization processes, including magma recharge (Bohrson & Spera, 2001, 2003), predicts more complex, non-linear relationships between the amount of assimilation and the extent of fractional crystallization.

Kerr *et al.* (1995) showed that lavas in the lower part of the Mull Plateau Group (part of the Palaeocene–Eocene North Atlantic Large Igneous Province; e.g. Saunders *et al.*, 1997) could be divided into two broad compositional groups: high-MgO (>8 wt %) basalts with high Ba and K, and low-MgO (<8 wt %) basaltic-hawaiites with low Ba and K. Isotope data show that the high-MgO lavas have the highest $^{87}Sr/^{86}Sr$ and Ba/Nb and the lowest $^{143}Nd/^{144}Nd$ and $^{206}Pb/^{204}Pb$, indicating assimilation of up to ~5% of felsic veins within Lewisian lower crustal granulites (Fig. 1). Huppert & Sparks (1985) suggested that primitive, hotter mafic magmas flowing turbulently through conduits could assimilate significant amounts of crust with little accompanying crystallization, such that the more primitive samples within a magmatic suite would show greater evidence for crustal assimilation than the cooler and more evolved samples. Kerr *et al.* (1995) proposed that such a mechanism (ATA; assimilation during turbulent ascent) could explain the compositional variations within the earliest lavas on Mull.

In this study, we analysed olivine-hosted melt inclusions in the high-MgO Mull Plateau Group lavas to investigate crustal assimilation processes and to assess the potential effects of post-eruptive alteration processes on the whole-rock compositions. Whole-rock compositions of lava flows represent averaged views that do not reflect the wider compositional diversity likely to have been present throughout the magmatic system, owing to the amalgamation and mixing of smaller, compositionally distinct, magma batches prior to or during eruption. Whole-rock compositions have also potentially been modified by the pervasive low-grade metamorphism that affects the Mull lava pile (e.g. Bailey *et al.*, 1924; Walker, 1970; Morrison, 1978). Crystals and their melt inclusions often record a greater diversity of magmatic compositions, thereby providing more detailed information about the magmatic system. One approach has been to look at isotopic variations in single crystals, usually Sr and Pb isotopes in plagioclase (Davidson *et al.*, 2007). Font *et al.* (2008) used this method to evaluate crustal assimilation in coeval lavas from the Isle of Skye (~100 km north of Mull: Fig. 2), but they had to focus

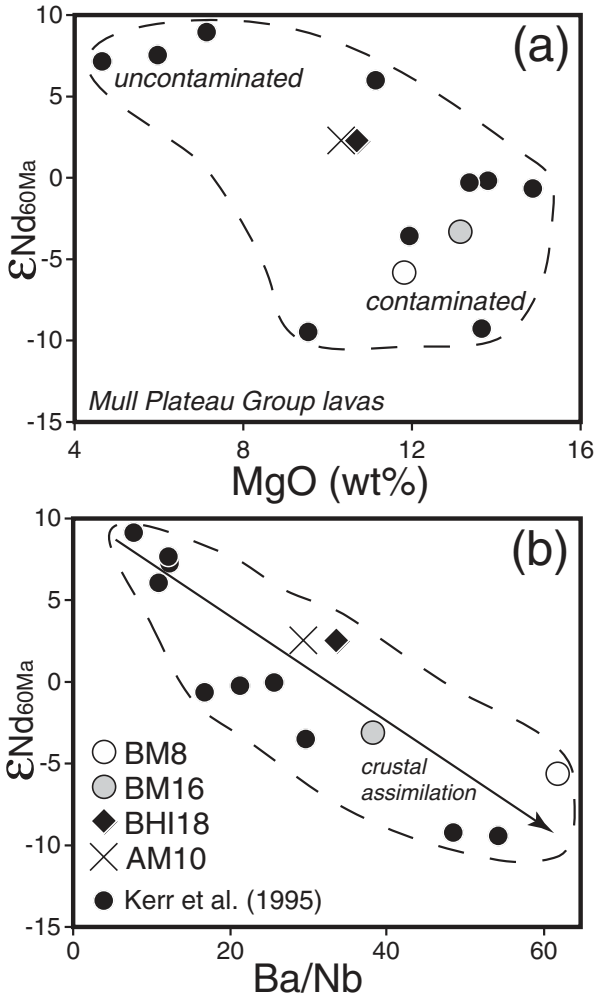

Fig. 1. Compositional and Nd isotopic variations in Mull Plateau Group lavas (Kerr *et al.*, 1995; this study), showing the greater crustal influence in the high-MgO samples as indicated by high Ba/Nb and low εNd_{60Ma}. (a) MgO vs εNd_{60Ma}, (b) Ba/Nb vs εNd_{60Ma}.

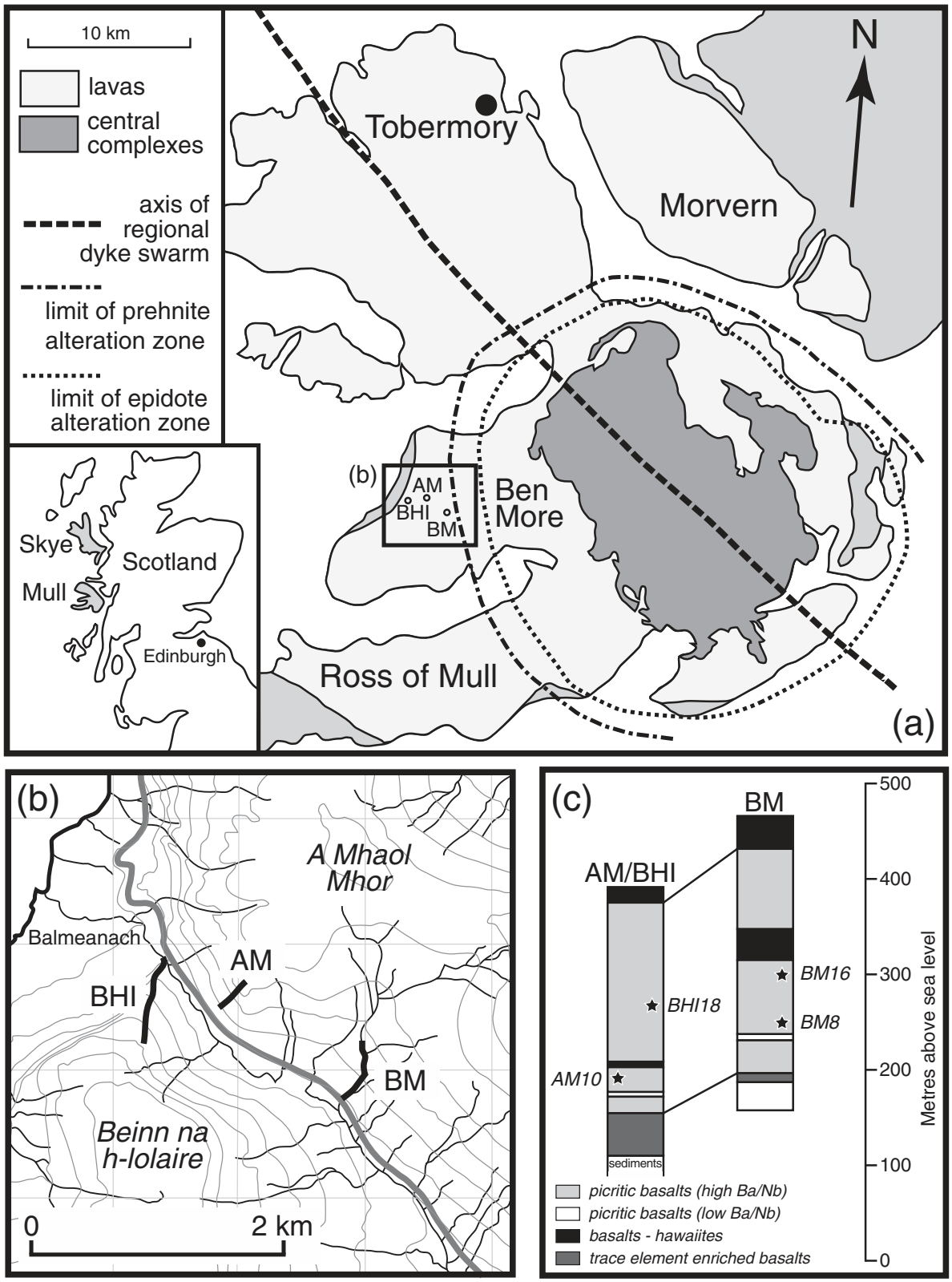

Fig. 2. (a) Simplified geological map of Mull showing the locations of the studied samples (after Kerr *et al.*, 1999) and the zone of low-grade metamorphism associated with the Central Complexes. (b) Detailed location map of the sampled sections. Thin grey horizontal and vertical lines are UK Ordnance Survey 1 km grid lines; thick grey line is the B3085 road. (c) Stratigraphic logs of sampled sections (from Kerr, 1995*a*).

on the more differentiated, plagioclase-bearing lavas. Olivine is the dominant phenocryst phase in the high-MgO Mull Plateau Group lavas, and olivine is not as amenable to similar isotopic studies owing to the incompatibility of Sr and Pb in its crystal structure. Olivines routinely host inclusions of melt trapped as the crystal grows, and these melt inclusions may preserve a wide diversity of compositions that can reflect the changing composition of the magma during crystallization (e.g. Kent, 2008). Several studies (e.g. Kent *et al.*, 2002; Yaxley *et al.*, 2004) have demonstrated the potential for using olivine-hosted melt inclusions to provide a high-fidelity record of crustal assimilation processes in flood basalt lavas. Melt inclusions are also given some protection against the effects of low-grade metamorphism by their host olivine crystal and thus may provide a means to recover magmatic compositions, especially for fluid-mobile elements such as K and Na (e.g. McDonough & Ireland, 1993; Kamenetsky *et al.*, 2004; Kent, 2008).

Reconnaissance data on olivine-hosted melt inclusions from the Mull Plateau Group lavas (Jones, 2005) showed significant trace element variations among melt inclusions from single samples that were interpreted to result from variable extents of crustal assimilation. These data were obtained using the Halter *et al.* (2002) approach in which laser ablation inductively coupled plasma mass spectrometry (LA-ICP-MS) analysis of whole crystallized inclusions is used to produce an average composition of the melt inclusion. This method does not allow detailed characterization of the major element and volatile content of the melt inclusions, making it more difficult to assess the fidelity of the compositional data from single melt inclusions (Nielsen *et al.*, 1998). We have carried out a more detailed study of olivine-hosted melt inclusions in four high-MgO (>8 wt %) Mull Plateau Group lava samples, using furnace homogenization techniques that allow single melt inclusions to be analyzed for major and trace elements and volatile contents. These new compositional data are used to assess the effects of low-grade metamorphism on whole-rock compositions and the timing of crustal assimilation and melt aggregation processes relative to growth of olivine crystals.

BACKGROUND GEOLOGY AND SAMPLE DETAILS

The Mull igneous complex consists of a central region of mafic and felsic intrusive rocks (cone sheets, ring dykes, larger intrusive complexes) surrounded by lava sequences (up to ~1 km thick) that cover an area of ~840 km^2 (Fig. 2; e.g. Bailey *et al.*, 1924; Kerr, 1995*a*). A flow-by-flow compositional sampling strategy revealed three main successive magma types within the lava pile (Kerr, 1995*a*, 1995*b*): Mull Plateau Group, Coire Gorm, and Central Mull Tholeiites. The Mull Plateau Group lavas, the focus of this study, form the lowermost ~730 m of the lava pile and comprise mildly alkaline basaltic rocks with steep light rare earth element (LREE) enriched chondrite-normalized patterns. The Mull Plateau Group lavas were erupted between $60{\cdot}6 \pm 0{\cdot}3$ Ma and $58{\cdot}7 \pm 0{\cdot}3$ Ma (^{40}Ar–^{39}Ar: Chambers & Pringle, 2001). The Coire Gorm lavas have essentially flat chondrite-normalized REE patterns and overlie the Mull Plateau Group lavas. The Central Mull Tholeiites, the youngest group, are more depleted in incompatible trace elements than the preceding types, with flat to LREE-depleted chondrite-normalized patterns.

Four representative samples of high-MgO lavas (BM8, BM16, BHI18, AM10; 10–13 wt % MgO) were selected based on the presence of relatively fresh olivines that contained melt inclusions. The high-MgO Mull Plateau Group basalts contain olivine phenocrysts set in a groundmass of plagioclase laths, subophitic clinopyroxene and interstitial FeTi-oxides (Fig. 3; Kerr, 1998). Intrusion of the Central Complexes led to the establishment of hydrothermal systems within the surrounding lavas that produced zones of alteration in the lava successions that decrease in intensity away from the Central Complexes (Fig. 2). The samples come from sections that show limited hydrothermal alteration (Kerr *et al.*, 1995). Whole-rock major and trace element compositions are provided in Table 1, with sample locations shown in Fig. 2.

ANALYTICAL METHODS

Olivine grains (~1 mm) were handpicked from coarse-crushed material. The presence of melt inclusions was evaluated visually by immersing the grains in ethanol and using a high-powered petrographic microscope. Petrographic observations confirmed that the melt inclusions were mostly to completely crystalline and therefore had to be rehomogenized to a glass prior to analysis. Groundmass-free olivine grains were reheated in a 1 atm Deltech vertical-tube gas-mixing furnace at the University of Iowa. Furnace temperatures were estimated from whole-rock compositions (BM8 1303°C; BM16 1312°C; BHI18 1270°C; AM10 1302°C), based on liquidus calculations from both COMAGMAT (Ariskin, 1999) and MELTS (Ghiorso & Sack, 1995). The oxygen fugacity was maintained slightly below the QFM (quartz–fayalite–magnetite) oxygen buffer in the sealed tube with a CO_2–H_2 gas mixture to prevent oxidation of the olivine grains. Samples were held at the calculated run temperature for ~10 min, with the total duration of heating above 1000°C kept to ~15 min, based on the methods and rationale discussed by Rowe *et al.* (2006, 2007). Samples were then rapidly quenched in a water bath, which resulted in glassy

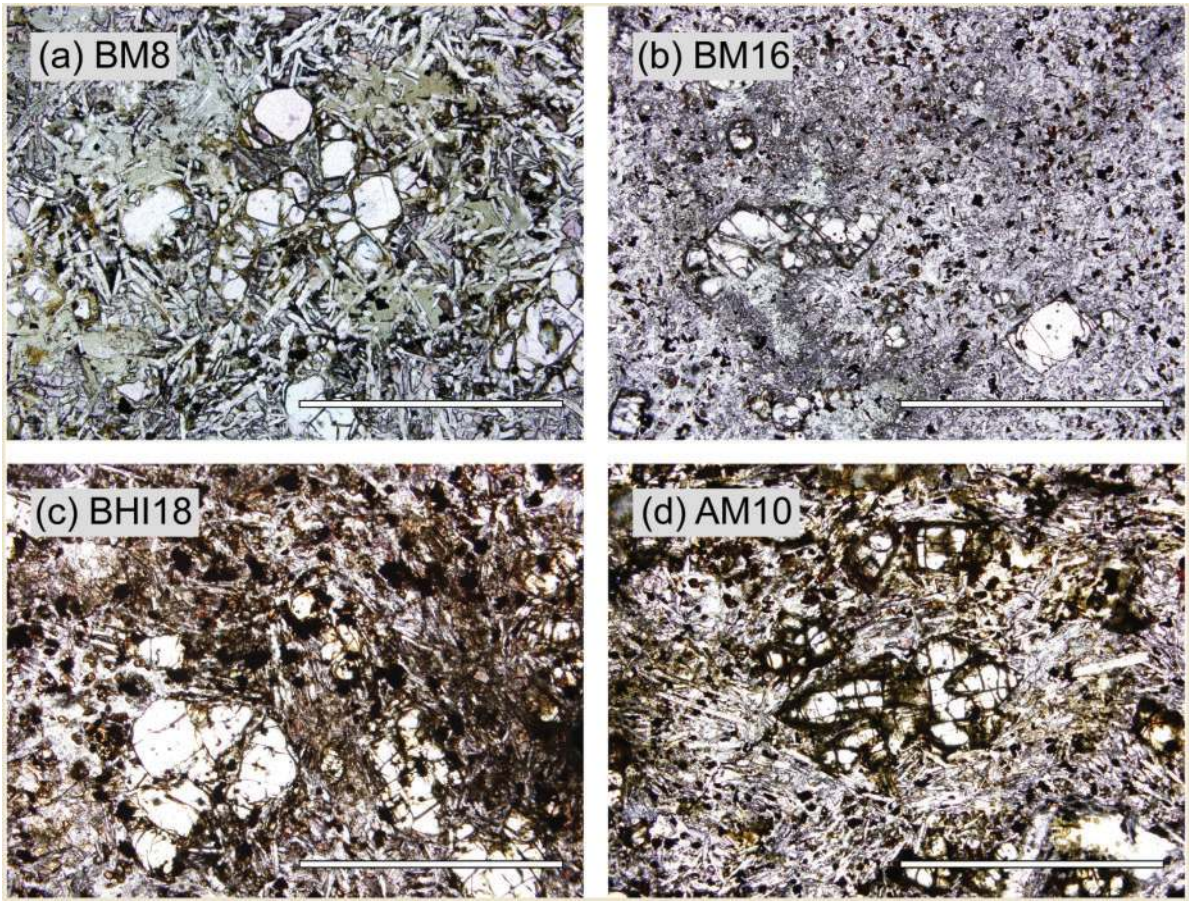

Fig. 3. Thin-section photographs of the four studied samples (plane-polarized light, 4×). White scale bar represents 2 mm.

melt inclusions. Olivine crystals were individually mounted in Crystalbond™ and polished to expose the melt inclusions. The crystals were then removed from the temporary Crystalbond™ mounts, and remounted with epoxy in groups of 10–20 crystals in 0·2 inch diameter Al-tubing. Six of these tubes were mounted into a 1 inch diameter round brass holder ready for *in situ* analysis.

Major element compositions of melt inclusions and host olivine crystals were measured using a Cameca SX100 electron microprobe at Oregon State University, following the analytical procedures described by Rowe *et al.* (2007). Olivine grains were analyzed using a focused (1 μm) beam with a 15 kV accelerating voltage and a 50 nA beam current. Melt inclusion analyses were obtained using a beam diameter of 4–7 μm (depending on inclusion size), with a 15 kV accelerating voltage and a 30 nA beam current. Mineral standards (San Carlos olivine: USNM 11312/444) and glass standards (BHVO-2 G, BCR-2 G, Loihi glass LO-02-04II) were analyzed repeatedly; the standard data are provided in Supplementary Data Tables A1 and A2 (available for downloading at http://www.petrology.oxfordjournals.org), respectively.

Trace element analyses of selected melt inclusions were carried out by secondary ion mass spectrometry (SIMS) at Arizona State University on a Cameca 6f instrument, using the analytical procedures described by Rowe *et al.* (2011). A $^{16}O^-$ primary beam (0·8–1·2 nA) focused to a ~20–25 μm diameter beam was used, and measured ratios ($M^+/^{30}Si^+$) were corrected for interfering oxides. For small inclusions, CaO concentrations calculated from $^{42}Ca/^{30}Si$ ratios were compared with the electron microprobe CaO analysis. If the SIMS CaO value was lower than expected, it is inferred that the beam had overlapped the host olivine, and trace element concentrations were corrected assuming a straight dilution of the melt composition. The robustness of these corrections can be assessed by comparing SIMS and electron microprobe analyses of Ti. The agreement between these two techniques is better than 18% for all inclusions, and better than 10% for 16 out of the 20 inclusions analysed by SIMS. The BHVO-2 G glass was used as a calibration standard, and the BCR-2 G glass standard was repeatedly run as an unknown to assess accuracy and precision (see Supplementary Data Table A3).

Major element compositions of the whole-rock samples were determined using a Jobin Yvon Ultima 2 inductively

Table 1: Whole-rock major and trace element data and Nd isotope data for the studied Mull Plateau Group lavas

Sample:	BM8	BM16	BHI18	AM10
Grid ref.:	NM974902	NM081156	NM298391	NM960472
SiO_2	47·27	46·99	46·49	46·30
TiO_2	1·29	1·37	1·71	1·81
Al_2O_3	15·48	14·20	15·58	15·68
FeO*	11·64	11·19	12·10	12·26
MnO	0·17	0·17	0·18	0·18
MgO	11·88	13·13	10·88	10·32
CaO	9·41	9·87	9·79	10·32
Na_2O	2·46	2·61	2·81	2·60
K_2O	0·27	0·29	0·26	0·33
P_2O_5	0·13	0·18	0·20	0·21
LOI	3·04	3·07	2·64	0·82
Total	100·14	100·81	100·45	99·36
Sc	31	31	29	28
V	260	277	289	265
Cr	950	920	296	368
Ni	446	341	255	316
Cu	67	124	116	103
Zn	75	81	91	90
Ga	15·5	16·6	18·1	18·4
Rb	4·2	4·8	3·5	3·5
Sr	216	294	436	362
Y	18·6	19·9	21·4	19·3
Zr	61·7	109	126	113
Nb	2·38	3·95	4·55	4·06
Cs	0·25	0·08	0·11	0·11
Ba	147	151	153	119
La	5·46	8·00	7·24	6·43
Ce	13·10	19·93	19·31	17·25
Pr	1·95	3·02	3·14	2·80
Nd	9·48	14·62	16·18	14·41
Sm	2·74	3·85	4·55	4·09
Eu	1·00	1·32	1·59	1·45
Gd	3·21	3·99	4·66	4·22
Tb	0·55	0·64	0·73	0·66
Dy	3·43	3·79	4·22	3·79
Ho	0·69	0·73	0·80	0·72
Er	1·92	2·01	2·15	1·92
Yb	1·77	1·79	1·85	1·66
Lu	0·26	0·26	0·27	0·24
Hf	1·71	2·75	3·22	2·93
Ta	0·12	0·20	0·24	0·22
Pb	1·06	1·44	1·16	1·05
Th	0·34	0·37	0·35	0·31
U	0·04	0·12	0·10	0·09
$^{143}Nd/^{144}Nd_m$	0·512339	0·512462	0·512755	0·512751
$^{143}Nd/^{144}Nd_i$	0·512270	0·512400	0·512688	0·512684
ε_{Nd} 60 Ma	−5·7	−3·2	2·4	2·4

coupled plasma optical emission spectrometer at the University of Cardiff, with the RF power set at 1000 W. Rock powder (0·1 g) was mixed with a lithium tetraborate flux (0·4 g) and several drops of lithium iodide wetting agent, and fused in platinum crucibles. The molten sample was dissolved in 50 ml of 6% HNO_3, spiked with 1 ml of a 100 ppm Rh solution as an internal standard, and diluted to 100 ml with deionized water. The data were calibrated relative to accepted values for a suite of rock standard reference materials (PCC-1, DTS-1, BIR-1, W-2, RGM-1, JA2, JA3, STM-1). The BIR-1 standard reference material was analysed as an unknown repeatedly during the analytical session and these data can be used to assess accuracy and precision (see Supplementary Data Table A4).

Trace elements in the whole-rock samples were analysed by ICP-MS using a Thermo X-series II instrument at the University of Iowa. Rock powder (0·1 g) was digested with HF–HNO_3, and run in 2% HNO_3 at a dilution factor of 5000, after spiking with internal standards (Be, Rh, In, Re, Bi). Data reduction included corrections for machine drift, reagent blanks, oxide interferences and isotopic overlaps. The data were calibrated with four rock standard reference materials (BHVO-2, BCR-2, AGV-2, BIR-1), using the preferred values from the GeoReM database (http://georem.mpch-mainz.gwdg.de/). Precision and accuracy were assessed from replicate analyses of standard reference materials analysed as unknown samples [see Peate *et al.* (2010) for replicate analyses of BRP-1 and JA-1 analyzed at the same time as the Mull lavas]. The accuracy relative to the GeoReM preferred values is <5% for all elements except Cr, Ni, Th, Ta and Nb. The precision (2 RSD) of replicate analyses is <3% for all elements except Rb, Y, La and Ga (<5%), and Sc, Cr, Cs, Th and U (<12%).

For Nd isotope analysis, whole-rock powders were digested with HF–HNO_3–HCl acids. REE were separated by cation exchange (AG 50Wx8 resin), and Nd was isolated from other REE using Eichrom Ln-spec resin. Nd isotope compositions were analysed by multi-collector (MC-)ICP-MS on the Nu Plasma instrument at the University of Illinois at Urbana–Champaign, using a $^{146}Nd/^{144}Nd$ value of 0·7219 to correct for instrumental mass fractionation. The Ames Nd metal standard was used to estimate reproducibility (±0·000011; 2 SD, $n = 9$), and the $^{143}Nd/^{144}Nd$ data are presented relative to an Ames Nd metal $^{143}Nd/^{144}Nd$ value of 0·51213 (equivalent to a La Jolla Nd standard $^{143}Nd/^{144}Nd$ value of 0·51185). Accuracy was assessed by analysing the JNdi-1 Nd standard and the BHVO-2 USGS rock standard. The JNdi-1 standard gave $^{143}Nd/^{144}Nd = 0·512107$, identical to the expected value (Tanaka *et al.*, 2000), and BHVO-2 gave $^{143}Nd/^{144}Nd = 0·512958$, within the range of published data (GeoReM: http://georem.mpch-mainz.gwdg.de/).

RESULTS

Compositions of the host olivine

Electron microprobe analyses of all olivine host crystals are provided in Supplementary Data Table A1. The compositional range of olivines for each sample is illustrated in Fig. 4. Samples BM8 and BM16, with the highest whole-rock MgO contents (12–13 wt %), have olivine compositions of $Fo_{85·8}$ to $Fo_{89·6}$ ($n = 24$), although BM16 contains a few olivines with lower forsterite contents ($Fo_{81·4}$ to $Fo_{84·5}$). Samples BHI18 and AM10 have lower whole-rock MgO contents (~10 wt %) and olivine compositions with correspondingly lower forsterite contents ($Fo_{80·6}$ to $Fo_{84·8}$; $n = 29$). NiO shows a positive correlation with Fo%, with an abundance of ~0·35 wt % at Fo_{90} and ~0·25 wt % at Fo_{81}. All olivines have CaO > 0·25 wt %, consistent with a magmatic origin rather than as mantle xenocrysts (e.g. Larsen & Pedersen, 2000). These data are consistent with olivine compositions (histogram in Fig. 4) reported for the Mull Plateau Group lavas by Kerr (1998) and Sobolev *et al.* (2007).

Screening of melt inclusions and correction methods for major element compositions

Electron microprobe analyses of all melt inclusions are provided in Supplementary Data Table A5. It is necessary to critically evaluate to what extent these compositions represent that of the original trapped liquid. Cracks in the host crystal can be formed either during the eruption of the basalt and subsequent low-grade metamorphic events or during the laboratory rehomogenization process. Figure 3 shows that the olivine crystals are fractured and partly altered to serpentine, chlorite, and iddingsite. If any cracks intersect a melt inclusion, then this can allow external material and alteration products to modify the inclusion composition and allow degassing of volatiles from the inclusion. Nielsen *et al.* (1998) demonstrated that such modified and breached inclusions should be marked by low sulphur contents, and also by low and/or variable Na contents. Figure 5 shows that the melt inclusion compositions form two distinct populations, a main group ($n = 34$) with high S (>390 ppm) and high Na_2O (>2·1 wt %), and a second group ($n = 19$) with low S (<390 ppm) and low Na_2O (<2·2 wt %). This second group, labelled in Fig. 5 as 'low-Na inclusions', are inferred to have been breached and modified by alteration products, following the rationale described by Nielsen *et al.* (1998). Their anomalous nature is also indicated by their high FeO contents (up to 18·4 wt %). Studies of rehomogenized inclusions with anomalously high FeO suggest that this may result from magnetite dissolution, originating from oxidation of either the host olivine or microphenocrysts trapped during inclusion formation (Rowe *et al.*, 2006). Either way, these inclusions are not recording primary melt compositions, and they are not considered further in the discussion about the petrogenesis of these lavas, nor plotted in subsequent figures.

Melt inclusion compositions can also be modified after their entrapment in the host crystal, through both natural processes and those that occur during the laboratory rehomogenization. The main concerns for olivine-hosted melt inclusions are post-entrapment crystallization of olivine on the walls of the inclusions and Fe loss owing to re-equilibration between the inclusion and the host olivine (e.g. Danyushevsky *et al.*, 2000; Kent, 2008). The Fe–Mg

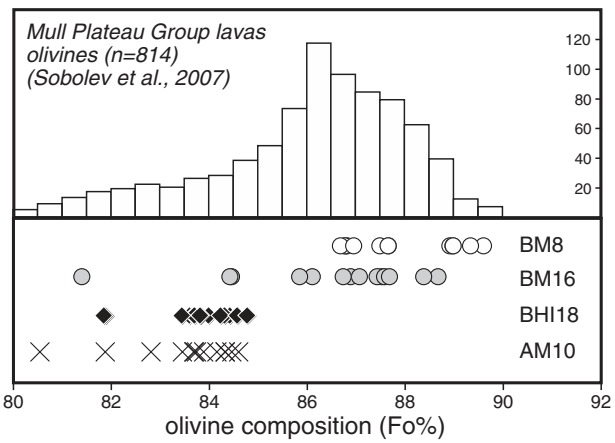

Fig. 4. Range in forsterite content of host olivine crystals in each sample (data from Supplementary Data Table A1). Histogram shows the distribution of olivine compositions ($n = 814$) from 14 samples of the Mull Plateau Group lavas (from Sobolev *et al.*, 2007).

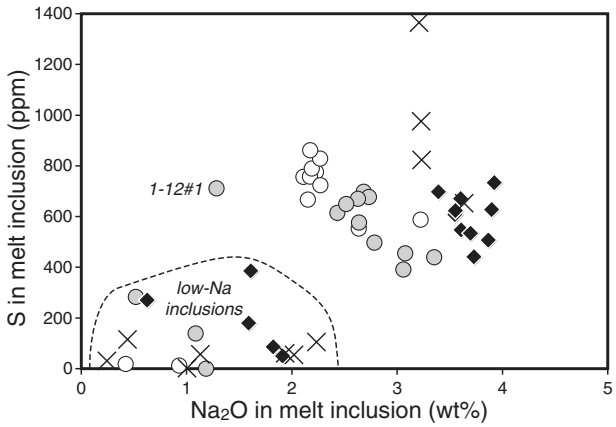

Fig. 5. S (in ppm) vs Na_2O (in wt %) for uncorrected melt inclusion compositions. Inclusions from each sample form a bimodal compositional distribution with a high-S, high-Na_2O group and a low-S, low-Na_2O group (labelled as 'low-Na inclusions'). Following Nielsen *et al.* (1998), the 'low-Na inclusions' are interpreted as breached inclusions whose compositions have been modified through exchange with the exterior. One inclusion (1-12#1) from sample BM16 is anomalous in having low Na_2O coupled with relatively high S, and its incompatible trace element composition is closer to that of the host whole-rock composition than the other melt inclusions in the sample. Symbols as in Fig. 4.

distribution coefficient (K_D^{Fe-Mg}) between each melt inclusion and its host olivine can be calculated and compared with the expected value for olivine–melt equilibrium ($K_D^{Fe-Mg} = 0{\cdot}30 \pm 0{\cdot}04$; Roedder & Emslie, 1970). If there has been minimal diffusive re-equilibration, then corrections for post-entrapment crystallization can be made by an iterative method in which olivine in equilibrium with the trapped melt is added progressively to the melt until equilibrium between the melt inclusion and the host olivine is reached. The extent of diffusive re-equilibration (Fe loss; Danyushevsky *et al.*, 2000) can be monitored by comparing the measured FeO content of each melt inclusion with its calculated K_D^{Fe-Mg}. Fe loss will produce a negative correlation between FeO and K_D^{Fe-Mg} for inclusions from a particular sample, and the program of Danyushevsky *et al.* (2000) can be used to correct for this Fe loss, assuming that the FeO contents of the inclusions are the same as the whole-rock value, after taking into account olivine accumulation. This assumption might not be strictly true for the Mull lavas because incompatible trace element data suggest that some of the whole-rocks have experienced greater extents of crustal assimilation than the melt inclusions (see below), which could potentially mean that the original FeO contents of the trapped inclusions would not be equivalent to the measured whole-rock FeO content. Although these correction procedures can lead to uncertainties in estimated FeO and MgO concentrations in the melt inclusions, they have minimal effect on the relative abundances of elements incompatible in olivine, and so data interpretations will largely focus on variations in incompatible elements.

Corrected major and trace element compositions of melt inclusions

Corrected major element compositions of unbreached melt inclusions are given in Table 2. Variations of selected major elements are shown in Fig. 6. Melt inclusions within single samples in general show relatively limited compositional variations. Melt inclusions from samples BM8 and BM16 have lower K_2O contents than the whole-rock samples, whereas melt inclusions from samples BHI18 and AM10 have lower SiO_2 and higher Na_2O than the whole-rock samples.

A subset of 20 melt inclusions from three samples (BM8, BM16, BHI18) were analysed for selected trace elements by SIMS (Table 3). There is a systematic increase in the contents of the more incompatible trace elements (e.g. Sr, Zr; Fig. 6e and f) in melt inclusions from sample BM8 to BM16 to BHI18, consistent with the whole-rock variations (Table 1). This increase is less pronounced for the less incompatible trace elements (e.g. Y), such that ratios of more incompatible to less incompatible elements also increase from sample BM8 to BM16 to BHI18.

Trace element compositions of the single melt inclusions are compared with the host whole-rock composition on primitive-mantle-normalized diagrams for each sample in Fig. 7. For samples BM16 and BHI18, most melt inclusions have similar normalized trace element patterns to the whole-rock, with the exception of Ba (and La in BM16), which is significantly enriched in the whole-rock analysis. For sample BM8, most melt inclusions are significantly depleted in the more incompatible elements (Th to Zr) compared with the whole-rock composition, and these include large ion lithophile elements (LILE; Ba, Sr, K), high field strength elements (HFSE; Nb), and LREE (La, Ce, Nd).

The sulphur, chlorine and fluorine contents of the melt inclusions were measured by electron microprobe. Detection limits for S, Cl and F (estimated at 140 ppm, 140 ppm, and 90 ppm respectively) were higher than usual owing to problems with one spectrometer. Measured Cl contents were all <250 ppm, whereas F contents were <200 ppm and only consistently detected in inclusions from the more evolved sample BHI18. Sulphur contents typically averaged between 600 and 800 ppm (BM8 798 ± 85 ppm; BM16 599 ± 113 ppm; BHI18 631 ± 88 ppm), with higher values in sample AM10 (900 ± 239 ppm).

DISCUSSION

Using melt inclusions to 'see through' the effects of whole-rock alteration

The Mull lava pile was affected by two types of low-grade metamorphic alteration (e.g. Walker, 1970; Morrison, 1978). Hydrothermal systems associated with the intrusive Central Complexes produced a metamorphic aureole of steeply dipping greenschist-facies to prehnite-facies zones (Fig. 2) marked by ^{18}O-depleted values in the altered lavas (e.g. Forester & Taylor, 1976). Away from this central region, the lava pile is marked by flat-lying zeolite-facies zones parallel to the base of the lavas, with most preserved flows in the laumontite zone (e.g. Walker, 1970). The analysed samples are from the Ben More area (Fig. 2), which straddles the region affected by the hydrothermal alteration around the Central Complexes. Although the samples show little petrographic evidence for significant alteration, the effects of minor alteration are pervasive and variable (Fig. 3). Of the primary magmatic phases, olivines show some minor, variable alteration to serpentine, chlorite and iddingsite, whereas microphenocrysts and groundmass clinopyroxenes and plagioclase feldspars show no alteration. Patches of former interstitial groundmass glass are altered to chlorite, which is particularly widespread in sample BM8 (Fig. 3a). The whole-rock samples all have high loss on ignition (LOI) values (3·0–4·5 wt %: Table 1), indicative of the presence of hydrated alteration minerals. Therefore, an important issue is the extent to which these alteration (± weathering) processes have modified the compositions of the lavas. As

Table 2: Corrected major element compositions of unbreached melt inclusions

Sample	Inclusion	SiO_2	TiO_2	Al_2O_3	FeO	MnO	MgO	CaO	Na_2O	K_2O	P_2O_5	S	Cl	F	Fo%	SIMS
BM8	1-02#1	46·88	0·92	15·20	11·60	0·13	11·58	11·38	2·03	0·09	0·08	786	bdl	bdl	86·8	✓
BM8	1-02#2	46·97	0·96	14·77	11·60	0·15	11·58	11·46	2·12	0·10	0·17	818	bdl	93	86·8	–
BM8	1-02#3	46·96	0·99	15·17	11·59	0·13	11·47	11·28	2·10	0·18	0·02	785	bdl	88	86·7	✓
BM8	1-03#1	46·40	0·88	13·77	11·60	0·09	15·06	10·19	1·79	0·05	0·03	802	155	bdl	89·6	✓
BM8	1-04#1	47·01	0·87	15·11	11·61	0·16	11·76	11·15	2·17	0·02	0·02	758	bdl	bdl	86·9	✓
BM8	1-05#1	47·28	0·62	14·52	11·60	0·09	14·05	8·88	2·76	0·05	0·02	685	235	bdl	88·9	–
BM8	2-02#1	46·56	0·74	14·19	11·60	0·08	14·65	9·75	2·21	0·03	0·04	661	151	bdl	89·3	–
BM8	2-03#1	46·65	0·90	14·83	11·60	0·14	12·30	11·34	2·05	0·05	0·01	843	bdl	bdl	87·5	✓
BM8	2-04#1	47·06	1·01	14·50	11·60	0·15	12·49	10·81	2·09	0·08	0·09	902	144	bdl	87·7	✓
BM8	2-04#2	46·46	0·97	14·86	11·60	0·12	12·49	11·29	2·00	0·05	0·04	936	bdl	bdl	87·6	✓
BM8	mean	46·82	0·89	14·69	11·60	0·12	12·74	10·75	2·13	0·07	0·05	798			87·8	
	± 1 s.d.	0·29	0·12	0·46	0·00	0·03	1·35	0·87	0·25	0·05	0·05	85			1·1	
BM8	*WR*	*47·27*	*1·29*	*15·48*	*11·64*	*0·17*	*11·88*	*9·41*	*2·46*	*0·27*	*0·13*					
BM16	1-02#1	46·45	1·42	14·48	11·11	0·08	11·21	12·12	2·53	0·22	0·27	602	bdl	197	86·9	✓
BM16	1-02#2	48·03	1·60	14·37	11·11	0·18	10·51	10·28	3·35	0·24	0·21	440	174	bdl	86·1	-
BM16	1-05#1	46·39	1·65	14·72	11·11	0·09	11·74	11·29	2·47	0·19	0·22	757	bdl	bdl	87·4	✓
BM16	1-06#1	46·62	1·69	15·19	11·11	0·09	10·29	11·73	2·67	0·22	0·28	693	238	95	85·8	✓
BM16	1-07#1	47·18	1·42	15·02	11·11	0·09	11·91	10·18	2·83	0·07	0·05	423	bdl	bdl	87·6	–
BM16	1-08#1	46·36	1·51	15·11	11·10	0·09	11·37	11·81	2·27	0·14	0·11	657	bdl	bdl	87·1	✓
BM16	1-08#2	46·66	1·54	16·04	11·11	0·11	9·25	12·25	2·60	0·18	0·13	677	170	bdl	84·5	✓
BM16	1-09#1	47·05	1·35	15·40	11·11	0·14	11·06	11·10	2·43	0·15	0·11	674	bdl	bdl	86·7	✓
BM16	1-11#2	45·81	1·33	13·82	11·12	0·07	13·18	11·60	2·45	0·11	0·39	565	105	bdl	88·7	–
BM16	1-11#3	46·51	1·34	12·98	11·11	0·09	12·81	11·92	2·79	0·13	0·19	502	236	bdl	88·4	–
BM16	1-12#1	48·00	1·49	16·99	11·11	0·23	7·51	12·40	1·52	0·56	0·08	598	bdl	bdl	81·4	✓
BM16	1-12#2	44·36	2·03	17·50	11·11	0·17	9·23	14·07	0·59	0·17	0·66	250	bdl	104	84·4	–
BM16	mean	46·71	1·49	14·71	11·11	0·10	11·33	11·43	2·64	0·17	0·20	599			86·9	
	± 1 s.d.	0·60	0·13	0·86	0·00	0·03	1·17	0·72	0·30	0·05	0·10	113			1·2	
BM16	*WR*	*46·99*	*1·37*	*14·20*	*11·19*	*0·17*	*13·13*	*9·87*	*2·61*	*0·29*	*0·18*					
BHI18	1-04#1	46·03	1·80	16·70	11·49	0·13	9·53	10·46	3·28	0·25	0·20	657	192	bdl	84·4	✓
BHI18	1-06#1	45·82	2·23	16·67	11·49	0·09	9·44	10·48	3·17	0·27	0·20	746	bdl	139	84·3	✓
BHI18	1-06#3	46·49	1·84	16·60	11·52	0·07	9·66	9·79	3·49	0·23	0·18	470	bdl	143	84·6	–
BHI18	1-07#1	45·67	1·98	16·74	11·50	0·12	9·47	10·14	3·64	0·32	0·30	538	bdl	186	84·3	–
BHI18	1-08#1	44·80	1·95	16·44	11·50	0·12	9·05	11·52	3·96	0·30	0·23	727	184	bdl	83·7	✓
BHI18	2-02#1	45·75	2·05	16·99	11·50	0·11	8·89	10·66	3·45	0·24	0·24	701	bdl	126	83·4	✓
BHI18	2-02#2	45·82	1·97	16·76	11·49	0·10	9·40	10·38	3·34	0·24	0·38	664	164	126	84·2	✓
BHI18	2-03#1	45·98	1·87	16·84	11·50	0·09	9·66	10·12	3·41	0·26	0·16	578	bdl	122	84·6	–
BHI18	2-03#2	46·16	1·94	16·39	11·51	0·11	9·81	9·95	3·42	0·35	0·24	576	143	152	84·8	–
BHI18	2-04#1	46·05	1·99	16·68	11·49	0·13	9·13	10·13	3·74	0·32	0·23	653	bdl	96	83·8	–
BHI18	mean	45·86	1·96	16·68	11·50	0·11	9·40	10·36	3·49	0·28	0·24	631			84·2	
	± 1 s.d.	0·44	0·12	0·18	0·01	0·02	0·29	0·49	0·23	0·04	0·06	88			0·4	
BHI18	*WR*	*48·09*	*1·68*	*15·04*	*11·66*	*0·17*	*10·55*	*9·54*	*2·85*	*0·23*	*0·17*					
AM10	1-01#1	42·05	1·51	21·40	11·59	0·14	8·97	10·12	3·55	0·24	0·30	886	145	bdl	83·5	–
AM10	1-02#1	45·99	1·87	16·63	11·60	0·16	9·75	9·74	3·58	0·29	0·28	663	156	103	84·6	–
AM10	1-06#1	45·45	1·13	17·73	11·59	0·18	7·41	12·23	3·56	0·29	0·31	1230	bdl	bdl	80·6	–
AM10	1-11#1	45·82	1·87	17·00	11·60	0·15	9·56	10·21	3·25	0·29	0·13	819	bdl	bdl	84·3	–
AM10	*WR*	*48·50*	*1·73*	*15·08*	*11·78*	*0·16*	*10·44*	*9·45*	*2·41*	*0·25*	*0·18*					

WR, whole rock composition from Table 1; bdl, below detection limit. Tick marks indicate inclusions analysed for trace elements by SIMS.

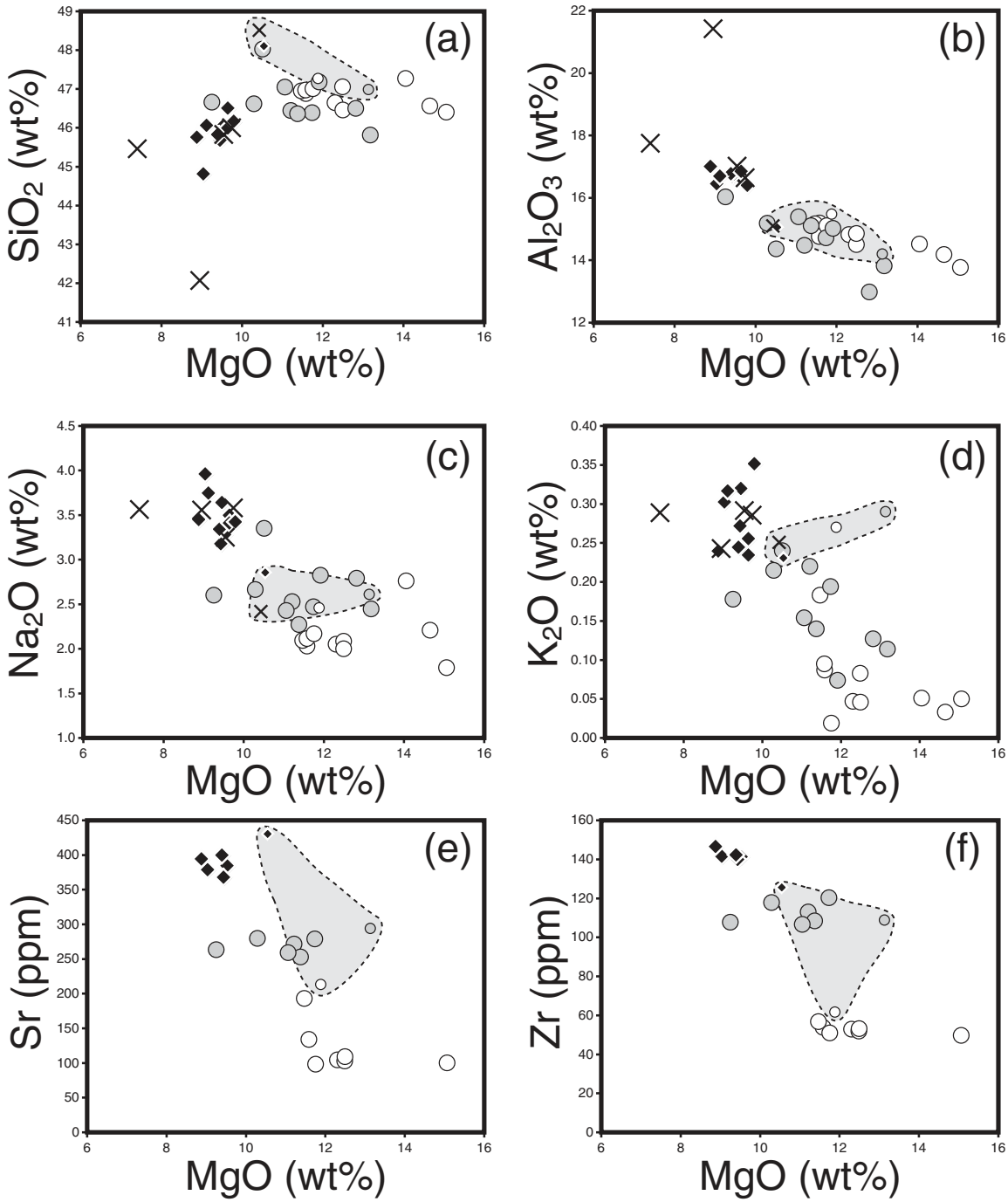

Fig. 6. Element variation diagrams for corrected melt inclusion data together with whole-rock compositions. MgO vs (a) SiO_2, (b) Al_2O_3, (c) Na_2O, (d) K_2O, (e) Sr, (f) Zr. Whole-rock compositions are shown with smaller symbols and outlined by the grey field. Symbols as in Fig. 4.

noted by Carmichael (2004), 'Unappealing as it might be, the Mull lavas are low-grade metamorphic rocks, and the chemical effects of a massive influx of water coursing through the lava pile cannot be ignored'. Studies on the Mull and Skye lavas have concluded that, whereas the HFSE (Ti, Zr, Nb, Y) and the REE were unaffected by the low-grade metamorphism, the LILE (e.g. K, Na, Rb, Ba, Sr) were variably mobilized (Humphris *et al.*, 1978; Morrison, 1978; Scarrow & Cox, 1995).

The compositions of melt inclusions protected inside olivines should be less susceptible to modification by the alteration processes that affected the host lava samples

Table 3: SIMS trace element data for Mull melt inclusions

Sample	Inclusion	Ti	Sr	Y	Zr	Nb	Ba	La	Ce	Nd	Sm	Gd	Dy	Yb	Th
BM8	1-02#1	5804	134	19·4	54	1·5	45	2·1	5·6	6·3	1·9	2·3	2·8	1·7	0·38
BM8	1-02#3	5770	193	20·1	57	1·5	97	3·6	9·9	7·9	3·3	2·5	3·5	1·8	0·90
BM8	1-03#1	5684	100	19·3	50	1·0	9	1·2	3·6	5·0	2·3	2·4	2·7	1·4	0·32
BM8	1-04#1	5413	98	17·6	51	1·0	10	1·0	4·1	5·4	2·6	3·1	3·0	1·4	–
BM8	2-03#1	5714	105	22·1	53	1·0	11	1·3	4·1	6·6	2·5	3·0	3·1	2·3	0·26
BM8	2-04#1	5605	103	19·5	52	1·4	10	1·2	4·6	5·9	2·4	3·1	3·0	1·9	0·25
BM8	2-04#2	6010	109	21·0	53	1·2	10	1·4	4·6	5·4	2·6	2·8	4·2	1·3	–
BM16	1-02#1	9299	271	22·4	113	3·8	64	5·9	19·2	13·0	4·2	3·1	3·7	1·7	0·31
BM16	1-05#1	9606	279	23·0	120	3·1	51	5·3	16·7	13·6	4·8	4·2	3·5	2·0	0·15
BM16	1-06#1	9324	280	22·4	118	3·7	65	6·4	19·3	15·2	3·9	3·9	4·3	1·6	0·63
BM16	1-08#1	9170	253	22·3	109	3·0	28	4·1	12·8	12·2	5·2	3·0	3·5	2·6	0·46
BM16	1-08#2	9317	264	23·2	108	2·9	25	3·8	14·7	11·2	3·5	3·5	4·3	1·6	0·17
BM16	1-09#1	9181	259	22·5	107	3·3	48	4·8	16·1	15·2	4·7	3·7	3·4	1·9	0·50
BM16	1-12#1	7928	308	19·9	102	3·0	114	7·1	20·4	13·3	4·5	3·1	4·5	2·3	–
BHI18	1-01#1	9362	151	19·4	105	2·8	37	3·2	10·6	11·3	4·2	2·9	3·6	2·6	0·09
BHI18	1-04#1	11528	384	23·3	141	4·4	83	6·6	18·9	16·7	5·4	4·4	4·6	1·3	0·44
BHI18	1-06#1	11270	367	22·1	140	4·3	73	5·9	18·0	15·9	4·2	3·6	3·9	1·8	0·46
BHI18	1-08#1	9588	378	20·2	141	4·2	80	5·8	16·3	17·7	4·4	4·5	3·4	1·4	0·86
BHI18	2-02#1	11737	394	25·3	146	4·9	75	5·8	18·7	16·8	4·3	4·0	3·7	2·6	0·39
BHI18	2-02#2	11410	399	23·0	142	4·9	94	6·8	21·0	17·8	5·7	4·6	4·7	1·5	0·51

(McDonough & Ireland, 1993; Kamenetsky *et al.*, 2004; Kent, 2008). Figure 8a compares the variations of two potentially mobile major elements, K and Na, between the unbreached, high-Na melt inclusions and the host whole-rock lava samples. The four whole-rock samples show a limited variation in both Na_2O (2·4–2·8 wt %) and K_2O (0·23–0·29 wt %). In contrast, the melt inclusions show a far greater variability (Na_2O 1·8–4·0 wt %; K_2O 0·02–0·35 wt %), but with a coherent positive correlation between Na and K. Melt inclusions within single samples show significant scatter, but there are systematic differences in melt inclusion composition between samples, and relative to the whole-rock compositions, that are significantly greater than the magnitude of the post-entrapment corrections (the correction procedures typically changed Na_2O and K_2O abundances by about 7%, and always less than 20%). Melt inclusions in samples BHI18 and AM10 have similar K_2O to the whole-rocks but higher Na_2O, whereas melt inclusions in sample BM16 have similar Na_2O to the whole-rocks but higher K_2O. Melt inclusions in sample BM8 have the lowest Na_2O and K_2O values of all the samples. In general, the whole-rock compositions of most Mull Plateau Group lavas plot above the trend shown by the melt inclusions, displaced to higher K_2O. Further evidence that the melt inclusions record magmatic values for mobile elements such as Na and K comes from systematic correlations with immobile trace elements such as the REE and Zr, Nb and Y. For example, the increase in $Na_2O + K_2O$ from sample BM8 to sample BM16 to sample BHI18 (Fig. 8b) is matched by an increase in the incompatible trace element ratios Zr/Y and La/Sm, indicative of a decrease in the extent of melting or a more incompatible trace element enriched mantle source (see below).

The variable mobility of Na and K affects the reliability of assigning lava samples to a particular magmatic lineage (tholeiitic, transitional, alkalic), based on whole-rock data. These classifications are based on the SiO_2–K_2O and SiO_2–Na_2O diagrams (Middlemost, 1975), the total alkalis–silica diagram (TAS; Le Bas *et al.*, 1986), and normative mineralogy (e.g. Tilley & Muir, 1962). Figure 8b shows the melt inclusion and whole-rock data on a TAS diagram (SiO_2 vs $Na_2O + K_2O$). Unlike the whole-rock compositions, the melt inclusions show a progressive increase in $Na_2O + K_2O$ from sample BM8 to sample BM16 to samples BHI18 and AM10. Whole-rock data for the studied samples all lie within the tholeiitic field, but melt inclusions from samples BHI18 and AM10 clearly plot in the alkaline field. These data indicate that Na but not K is significantly mobile during alteration of the alkaline

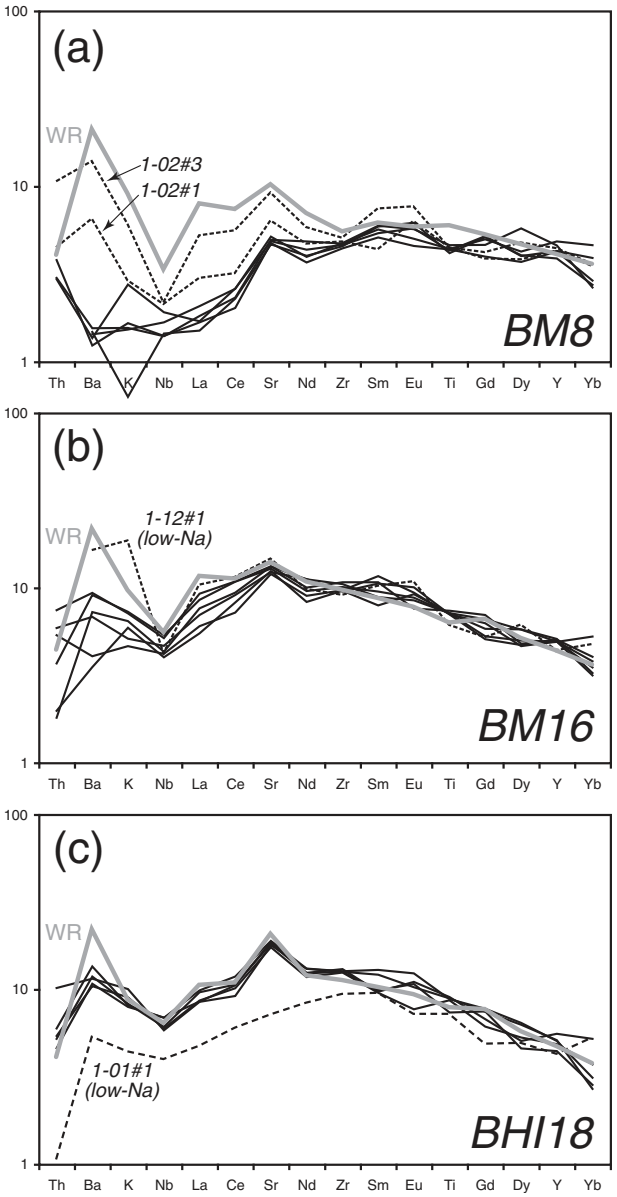

Fig. 7. Primitive-mantle-normalized plots of average melt inclusions for each sample compared with the respective whole-rock composition: (a) BM8; (b) BM16; (c) BHI18. Normalizing values from Sun & McDonough (1989). Whole-rock (WR) compositions are shown by the thick grey line. The main group of compositionally similar melt inclusions within each sample are shown by fine black lines; melt inclusions with more anomalous compositions are shown by fine dotted lines and labelled with the inclusion number.

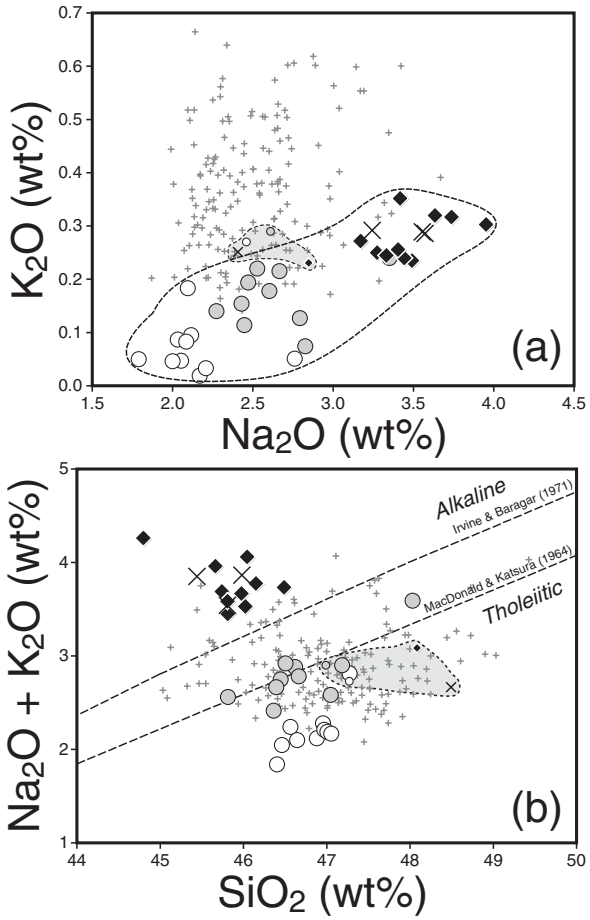

Fig. 8. (a) Na_2O vs K_2O and (b) total alkalis–silica classification diagram (SiO_2 vs Na_2O+K_2O; Le Bas *et al.*, 1986), showing whole-rock data and corrected melt inclusion data for high-S, high-Na melt inclusions. Whole-rock compositions are shown with smaller symbols and outlined by the grey field. Small grey cross symbols (+) are published whole-rock analyses of Mull Plateau Group lavas with similar MgO contents (9–14 wt %: Kerr *et al.*, 1995, 1999). Dashed lines mark the alkalic–tholeiitic divisions of Macdonald & Katsura (1964) and Irvine & Baragar (1971). Symbols as in Fig. 4.

samples (BHI18 and AM10), whereas $K \pm Na$ are mobile during alteration of the tholeiitic to transitional samples (BM8 and BM16).

Compositional characteristics of crustal assimilation in Mull lavas

The crustal structure beneath Mull comprises a lower–middle crust of Archaean Lewisian granulite- and amphibolite-facies gneisses overlain by Late Proterozoic Moine metasediments (Bailey *et al.*, 1924; Bamford *et al.*, 1977). These units are isotopically distinct, particularly in terms of Pb isotopes (Dickin, 1981; Kerr *et al.*, 1995; Preston *et al.*, 1998). Moine metasediments have high $^{206}Pb/^{204}Pb$ (>19), whereas Lewisian rocks all have low $^{206}Pb/^{204}Pb$ (<16), with the amphibolites distinguished from the granulites by their higher $^{208}Pb/^{204}Pb$. Isotopic data for the Mull Plateau Group lavas (Fig. 9a; Kerr *et al.*, 1995) show that they have been variably contaminated by Lewisian granulitic lower crust, and mass-balance arguments suggest that the assimilated material was a K-rich silicic partial melt of Lewisian leucogneiss (Thompson *et al.*, 1982; Kerr *et al.*, 1995). Peate *et al.* (2008) reviewed isotope data on Cenozoic igneous rocks from the North

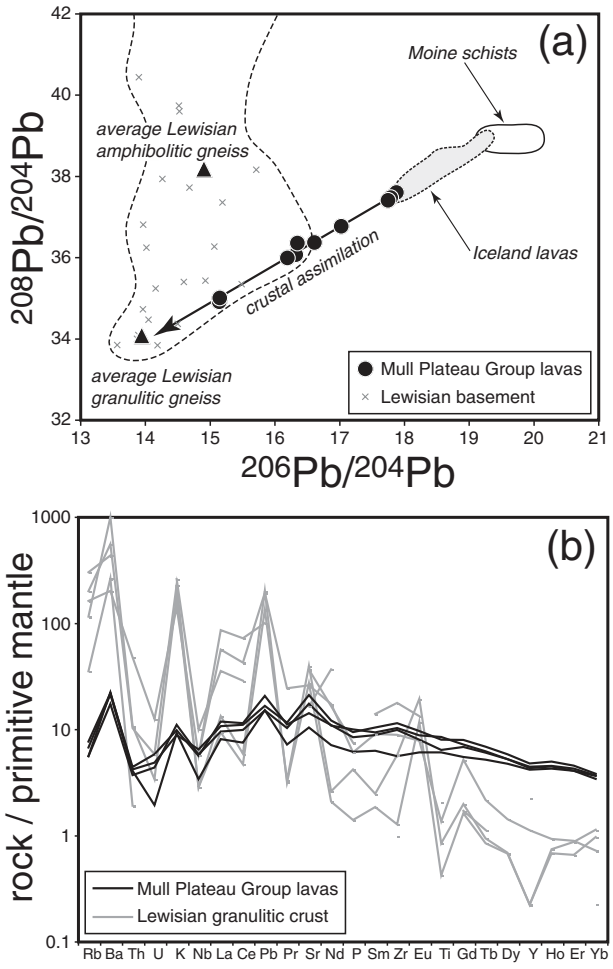

Fig. 9. (a) $^{208}Pb/^{204}Pb$ vs $^{206}Pb/^{204}Pb$ diagram showing that the Mull Plateau Group lavas were variably contaminated with Lewisian granulitic lower crust (Dickin, 1981; Whitehouse, 1990; Kerr *et al.*, 1995; Whitehouse & Robertson, 1995; Preston *et al.*, 1998). Field for Icelandic lavas indicated to represent uncontaminated mantle melts from Peate *et al.* (2010). (b) Primitive-mantle-normalized trace element patterns of Lewisian granulitic crust samples (Thompson *et al.*, 1982; Kerr *et al.*, 1995) and the four whole-rock lava compositions from this study (normalizing values from Sun & McDonough, 1989).

Atlantic region and showed that any basalt with $\varepsilon_{Nd} < +4$ was clearly contaminated with crustal material. The two alkaline samples (BHI18 and AM10) both have ε_{Nd} of +2·4, whereas the tholeiitic to transitional samples (BM8 and BM16) have lower ε_{Nd} of −5·7 and −3·2, respectively, which indicates that crustal assimilation was important in the evolution of all four samples.

The expected elemental signature of crustal assimilation by Lewisian granulites has been established from whole-rock studies of the Palaeogene Mull and Skye lavas, and analyses of local granulitic rocks (e.g. Thompson *et al.*, 1982; Kerr *et al.*, 1995). The most notable features are the large enrichments in K and Ba and lesser enrichments in Rb and Sr relative to Th and the HFSE (Fig. 9b). This has led to the use of enrichments of Ba relative to HFSE to screen for clearly contaminated lavas; for example, $Ba/Nb > 20$ (Kerr *et al.*, 1995), $Ba/TiO_2 > 90$ (Scarrow & Cox, 1995), $Ba/Zr > 2$ (Chambers & Fitton, 2000). The whole-rock compositions of the studied samples have elevated Ba/Nb ratios (29–62), suggestive of some crustal assimilation, using the $Ba/Nb > 20$ criterion of Kerr *et al.* (1995), consistent with the Nd isotope data (Fig. 1). Although Ba and K are the two most diagnostic elements for differentiating crustal assimilation by Lewisian granulitic gneisses (Thompson *et al.*, 1982; Kerr *et al.*, 1995), some caution is needed as these elements are also susceptible to mobilization by post-eruptive alteration. For example, melt inclusions in sample BHI18 have limited compositional variability and all have trace element compositions within error of the whole-rock composition, with the exception of Ba, which is elevated in the whole-rock data (Fig. 7c). The fact that the whole-rock analysis is otherwise the same as the trace element compositions of the melt inclusions indicates that some of the whole-rock Ba enrichment is the result of subsequent alteration. Despite the mobility of Ba during post-eruption alteration, the broad correlation between Ba/Nb and $^{143}Nd/^{144}Nd$ (Fig. 1b), an isotope ratio minimally affected by alteration (e.g. Hawkesworth & Morrison, 1978), shows that the Ba enrichment from crustal assimilation is still clearly resolvable in many Mull lavas.

The reconnaissance melt inclusion study on Mull Plateau Group lavas by Jones (2005) relied on the enrichment of Ba relative to Nb and Zr to quantify the extent of crustal assimilation in single melt inclusions, but the analytical technique used did not allow for the recognition of inclusions potentially modified by alteration that might affect Ba contents, as our study has revealed. We need a means to distinguish the effects of alteration versus crustal assimilation in the melt inclusions, and this will rely on selecting incompatible elements that are immobile during alteration but enriched in crustal materials. In many continental flood basalt provinces, Th enrichment relative to Nb or Ta is commonly used to assess the extent of crustal assimilation in lavas (e.g. Peate & Hawkesworth, 1996), but compared with most crustal assimilants, the Lewisian granulitic gneisses are rather unusual in being characterized by low Th contents (Fig. 9b; Thompson *et al.*, 1982; Kerr *et al.*, 1995). Enrichment of LREE relative to Nb and Ta (or other HFSE) is another common signature of crustal assimilation. Kerr *et al.* (1995) showed that this is indicative of the assimilation process that affected the Mull Plateau Group lavas (e.g. Fig. 9b). Furthermore, Humphris *et al.* (1978) showed that the LREE were immobile during alteration of the Mull lavas. Therefore, coupled enrichments of Ba and LREE relative to HFSE should be diagnostic of crustal assimilation in these melt inclusions.

Melt inclusion evidence for the relative timing of assimilation and crystallization

New constraints on the nature of the assimilation process in the Mull Plateau Group lavas come from looking at the compositional variability of melt inclusions within single samples as well as comparing their compositions with the whole-rock composition, as this demonstrates the timing of crustal assimilation relative to olivine crystallization. These comparisons are shown using primitive-mantle-normalized trace element patterns (Fig. 7). Melt inclusions in sample BM16 show more compositional scatter than those in sample BHI18, but still have patterns that are broadly similar to the whole-rock composition, although with lower Ba, K and La contents. Most inclusions in sample BM8 have significantly lower contents of the more incompatible trace elements (Th to Zr) compared with the whole-rock composition, but two inclusions (1-02#1 and 1-02#3) from the same olivine grain have compositions that are intermediate between those of the other melt inclusions and the whole-rock.

The relationship between melt inclusion and whole-rock compositions is explored further in Fig. 10a (Ce/Zr vs Ba/Zr), which evaluates enrichments in Ba and LREE relative to the HFSE. Zr was chosen as the HFSE and Ce as the LREE, which because of their higher abundances compared with Nb and La, respectively, are more precisely determined by SIMS analysis. Crustal assimilation models are plotted for samples BM8 and BM16 using a Lewisian granulite composition [average of samples 7 H (Thompson *et al.*, 1982) and P42 (Kerr *et al.*, 1995) that have suitable Ba/Ce values]. Melt inclusions in sample BHI18 have Ce/Zr values that scatter close to the whole-rock value, but at a significantly lower Ba/Zr value (~0·6 vs 1·2), consistent with subsequent alteration enrichment of Ba. Therefore, the crustal assimilation of the BHI18 magma, indicated by its relatively low ε_{Nd}, must have occurred prior to crystallization of the olivines that are present in the sample. For sample BM8, the whole-rock is significantly enriched in both Ce/Zr and Ba/Zr relative to all the melt inclusions. Two compositionally distinct melt inclusions (1-02#1 and 1-02#3) fall on a tie-line between the main group of inclusions (at low Ce/Zr and Ba/Zr) and the whole-rock (at high Ce/Zr and Ba/Zr). This trend is consistent with crustal assimilation, and constrains the assimilant Ba/Ce ratio to be ~15. The whole-rock has a significantly more contaminated composition than any of the melt inclusions, which indicates continued assimilation after crystallization of the olivines present in the sample. Melt inclusions in sample BM16 show some compositional variability in which Ce/Zr and Ba/Zr values are positively correlated, indicative of minor crustal assimilation concurrent with olivine crystallization. The whole-rock composition of sample BM16 plots at significantly higher Ba/Zr than the melt inclusions (1·4 vs ~0·5), and slightly higher Ce/Zr compared with the highest Ce/Zr inclusion, again suggestive of continued assimilation after the growth of the olivines in the sample, perhaps with some late-stage Ba enrichment from alteration. The exact amount of assimilation depends on the elemental concentrations of the initial magma and the crustal assimilant, neither of which are known. However, the amount of assimilation needed to explain the difference between the lowest Ba/Zr and Ce/Zr melt inclusion and its host whole-rock composition is similar for both BM8 and

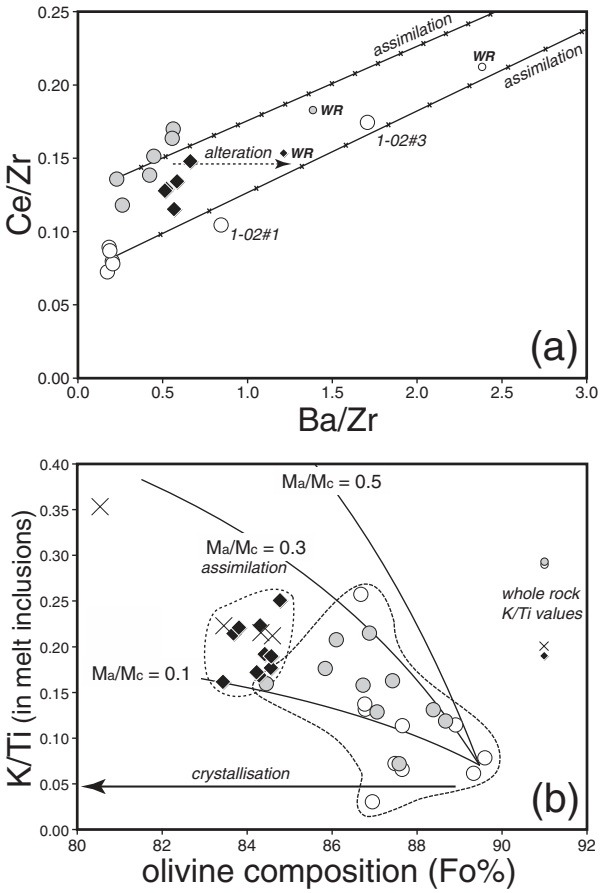

Fig. 10. (a) Ce/Zr vs Ba/Zr for melt inclusions and whole-rock samples, illustrating the contrasting vectors for alteration vs crustal assimilation. Crustal assimilation trends represent simple mixtures between the least contaminated melt inclusions in samples BM8 and BM16 with an average Lewisian granulite (average of samples 7 H and P42: Thompson *et al.*, 1982; Kerr *et al.*, 1995). (b) K/Ti in melt inclusions vs host olivine composition (Fo%). COMAGMAT modelling (Ariskin, 1999) at a range in pressures (1–10 kbar) and fO_2 values (QFM to QFM + 1) predicts no significant changes in melt K/Ti values during fractional crystallization. The continuous curved lines are calculated trends for coupled assimilation and fractional crystallization (AFC) of olivine starting from the most primitive melt inclusions in samples BM8 and BM16 respectively. Crust composition is an average Lewisian granulite composition (average of samples 7 H and P42; Thompson *et al.*, 1982; Kerr *et al.*, 1995), and trends are calculated for M_a/M_c (mass assimilated/mass crystallized) of 0·1, 0·3 and 0·5. Symbols as in Fig. 4.

BM16, assuming the same crustal assimilant composition. Although both samples BM8 and BM16 seem to indicate that there was continued assimilation after the trapping of the analysed melt inclusions in the olivine crystals, there is a potential bias in the studied melt inclusion population. The pervasive alteration of olivines in these samples (Fig. 3) means that the olivine fragments recovered during the mineral separation process might be biased towards the cores; melt inclusions in the outer altered rims that would have recorded later stages of olivine growth are less likely to have been preserved and sampled.

Additional information about the assimilation process can be inferred from the compositional variations in the melt inclusions of each sample as a function of magmatic differentiation (Fig. 10b). The host olivine composition (Fo%) is used as a differentiation index rather than the melt inclusion MgO content, because the correction procedures for post-entrapment modification lead to less well-constrained MgO contents (e.g. Kent *et al.*, 2002). The K/Ti ratio is used as a monitor of crustal assimilation, as K is strongly enriched relative to Ti in the Lewisian crustal assimilants (Thompson *et al.*, 1982; Kerr *et al.*, 1995). K and Ti are major elements that were measured by electron microprobe, and so there are more melt inclusion data available, as trace element analyses were made only on those inclusions big enough for SIMS analysis. Both elements are strongly incompatible in olivine and so variations in K/Ti are independent of any uncertainties introduced by the post-entrapment correction procedures. COMAGMAT modelling (Ariskin, 1999) at a range of pressures (1–10 kbar) and fO_2 values (QFM and QFM + 1) shows that the K/Ti ratio is insensitive to the effects of fractional crystallization until the appearance of FeTi oxides in the fractionating assemblage at MgO contents $\ll$6 wt %.

Melt inclusions from samples BHI18 and AM10, with one exception, have a limited range in host olivine compositions ($Fo_{83·4}$–$Fo_{84·8}$) and in K/Ti (0·16–0·25) that overlaps with the whole-rock values (K/Ti = 0·20; Fig. 10b). The limited variability in K/Ti in the melt inclusions is consistent with minor fluctuations in crustal assimilation during olivine growth. In contrast, melt inclusions from samples BM8 and BM16 both show broad trends of increasing K/Ti (0·03–0·26) with decreasing Fo% in the host olivines ($Fo_{89·6}$–$Fo_{84·5}$), although never reaching the values measured in the whole-rocks (K/Ti = 0·29). The three melt inclusions in sample BM8 with the highest K/Ti (>0·12) are all from the same olivine crystal, and trace element data from two of them show the highest Ba/Nb values in this sample (30–63 vs 7–11 in other melt inclusions). The broad trend shown by sample BM16 is largely defined by the three inclusions with the lowest K/Ti (<0·13) and the most forsteritic host olivines ($Fo_{87·6}$–$Fo_{88·7}$), but these were too small for trace element analysis by SIMS to determine Ba/Nb values.

The broad trend of increasing K/Ti in inclusions with decreasing forsterite content from the two more incompatible-element-depleted samples (BM8 and BM16) is consistent with an AFC style of crustal contamination (e.g. DePaolo, 1981; Kent *et al.*, 2002) in which the assimilation is accompanied by fractional crystallization. Following Kent *et al.* (2002), we modelled trajectories in Fig. 10b that represent assimilation of Lewisian granulitic crust during progressive olivine fractional crystallization of the most primitive melt inclusions in samples BM8 and BM16 for different relative amounts of assimilation compared with fractionation (M_a/M_c ratios of 0·1–0·5). Melt inclusions in both samples show enough scatter that the trends cannot be explained by a single M_a/M_c value. Some of the least contaminated melt inclusions in sample BM8 have approximately constant K/Ti values over a range in Fo%, indicating minimal assimilation during crystallization, whereas other inclusions require M_a/M_c values up to a maximum of about 0·3. A similar situation is seen in the sample BM16 melt inclusions, although some inclusions require slightly higher M_a/M_c values of up to 0·5. These estimates are lower than the inferred M_a/M_c values (>1–10) for melt inclusions in Yemen flood basalts by Kent *et al.* (2002).

Previous studies on flood basalt lavas (Kent *et al.*, 2002; Yaxley *et al.*, 2004) showed that olivine-hosted melt inclusions can record variable extents of crustal assimilation during entrapment. Melt inclusions in Paleocene picritic lavas from Baffin Island have compositions that require significantly greater amounts of crustal assimilation (~15%) compared with the host lavas (~1%). Yaxley *et al.* (2004) argued that this implied that crustal assimilation was taking place on a very localized scale on the walls of the magmatic storage–feeder systems, with melting of crustal lithologies coupled with rapid growth of new olivine crystals that were subsequently mixed into the main magma body where little olivine growth was taking place. This concept of localized assimilation was first introduced by Danyushevsky *et al.* (2003, 2004). Melt inclusions in Oligocene flood basalts from Yemen are highly diverse in composition, consistent with variable addition of crustal material of different compositions (Kent *et al.*, 2002). The large variations in incompatible element ratios sensitive to crustal assimilation (e.g. Ba/Nb and K/Nb) in melt inclusions trapped in olivines of similar forsterite compositions highlight the complexity of the assimilation history of an erupted lava and emphasize that a simple AFC model is not reasonable for such plumbing systems. In contrast to the Baffin Island case, the average melt inclusion composition for each Yemen sample is indistinguishable from the host lava composition. This indicates that the inclusions are sampling the full compositional diversity of melt batches within the magmatic plumbing system (including

relatively uncontaminated melts and highly contaminated melts) that eventually become homogenized to produce the host lavas. The Yemen samples contain highly contaminated melt inclusions trapped within highly forsteritic olivines ($Fo_{85–90}$) that require very high rates of crustal assimilation relative to crystal fractionation. Kent *et al.* (2002) argued that these inclusions sample highly contaminated zones adjacent to the margins of conduits or magma chambers, in which hot primitive melts are in contact with wall-rocks that have been heated close to their solidus. This could result from replenishment events bringing hot primitive magmas into locations where the wall-rocks have already been heated by pre-existing resident magma, or from turbulent flow in primitive magmas that will also lead to rapid heat transfer to the crustal wall-rocks (the ATA model of Kerr *et al.*, 1995). As thermal diffusion is faster than mass transport in a magma, the heat can be provided from a larger volume of magma than is involved in the boundary layer mixing.

In the case of the Mull lava samples studied here, the melt inclusions show similar or lower extents of assimilation compared with the host lavas, in contrast to the Baffin Island data of Yaxley *et al.* (2004), and they show less compositional diversity in terms of the extent of assimilation and the variability in the assimilant composition compared with the Yemen data of Kent *et al.* (2002). Within the Mull Plateau Group lavas, whole-rock analyses of the more primitive lavas (MgO > 8 wt %) show greater extents of crustal assimilation compared with the more evolved lavas (MgO < 8 wt %). Kerr *et al.* (1995) proposed an ATA (assimilation during turbulent ascent) mechanism to explain this observation. This was based on the modelling of Huppert & Sparks (1985) that indicated that primitive, hot mafic magmas could assimilate significant amounts of crust with little accompanying crystallization by virtue of the rapid transfer of heat to the wall-rock through turbulent flow through conduits. Kerr *et al.* (1995) argued that the more evolved lavas represent magmas that fractionated at sub-crustal depths, perhaps just below the Moho (~30 km), within the refractory uppermost lithospheric mantle. As a consequence, when these magmas eventually rose through the crust, they were too cool to assimilate much crustal material or too viscous to flow turbulently. In contrast, the more primitive lavas represent magmas that crossed the Moho without significant prior fractionation and therefore could ascend turbulently through the crust, resulting in significant crustal assimilation with limited crystallization.

In the two tholeiitic samples (BM8 and BM16) where the melt inclusions show significant compositional variability linked to crustal assimilation, the olivine compositions overlap with the highest forsteritic olivine compositions in the Mull Plateau Group lavas (Fig. 4), and indicate that the hottest magmas were, in fact, undergoing assimilation concurrently with olivine crystallization. It is notable that the extent of assimilation in these two samples broadly correlates with decreasing forsterite content of the host olivine, indicating an AFC style of assimilation with crustal material of similar composition. The overall evolution of the Mull Plateau Group suite follows an ATA style of crustal assimilation, but in detail, the process of assimilation within single magma batches at the length scale of olivine crystals follows an AFC-type mechanism.

Inferring primary melt compositions and magmatic temperatures from melt inclusions

The major element compositions of primitive magmas can be used to infer details about mantle melting conditions and source lithologies (e.g. Klein & Langmuir, 1987; Herzberg & Asimow, 2008), but care is needed in applying these methods to altered rocks such as the Mull Plateau Group lavas. Kerr (1995*b*) showed that the Mull Plateau Group lavas show broad correlations between $Na_{8·0}$ (Na_2O recalculated to 8 wt % MgO; Klein & Langmuir, 1987) and both $Si_{8·0}$ (negative) and $Fe_{8·0}$ (positive). These trends approximate the 'local' trends of Klein & Langmuir (1987) and suggest that the erupted lavas represent variable mixtures of melts derived from different levels within the melt column. However, Kerr (1995*b*) had to restrict this dataset to samples with MgO of 6–8·5 wt % because the more primitive lavas were more crustally contaminated (Ba/Nb > 20), which might have affected their major element compositions. Kerr (1995*b*) also showed crude negative correlations between the degree of silica saturation and incompatible element contents in these lavas (Fig. 11a). This observation is also consistent with a polybaric melting model in which basalts with higher incompatible element contents are more ne-normative and contain greater contributions from high-pressure, low-degree melts from the lower parts of the melting column, whereas basalts with lower incompatible element contents are more hy-normative and dominated by contributions from more extensive melting at shallower levels in the melting column. The considerable scatter in all these trends is probably due to the effects of alteration (Kerr, 1995*b*).

We have demonstrated that olivine-hosted melt inclusions provide more robust estimates of magmatic liquid compositions than whole-rocks for the potentially mobile alkali elements Na and K. Inclusions in Mull lavas preserve a wider range of Na_2O and K_2O values than the whole-rocks (Fig. 8), and show coherent trends between increased alkalinity ($Na_2O + K_2O$) and trace element indicators of lower extents of melting or a more fertile source, such as Zr/Y (Fig. 11b). The progressive increase in alkalinity from samples BM8 to BM16 to BHI18/AM10 is matched by an increase in Zr/Y, revealing a record of the

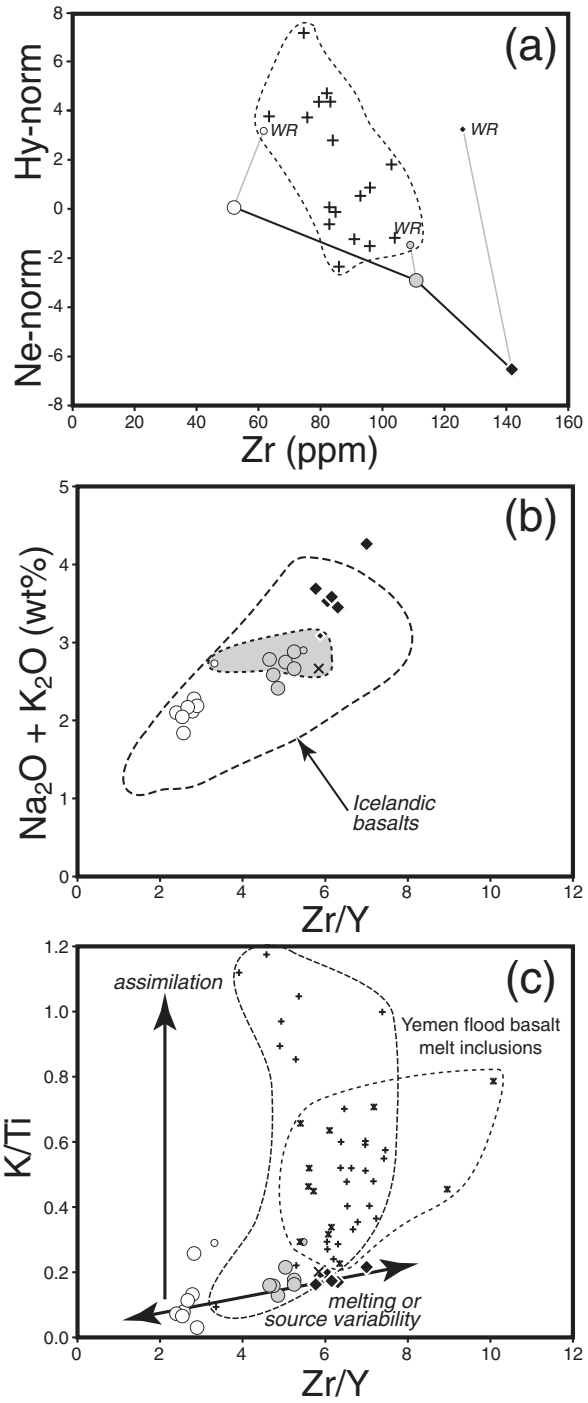

Fig. 11. (a) Zr vs silica saturation index. Melt inclusion (MI) data are plotted as averages. Crosses (+) represent Mull Plateau Group lava whole-rock (WR) data from Kerr (1995*b*). (b) $Na_2O + K_2O$ vs Zr/Y for the melt inclusions. Grey shaded field encloses the four whole-rock samples. Melt inclusions have compositions consistent with typical melts of North Atlantic mantle as represented by post-glacial Icelandic basalts (field outlined by dashed line; Sinton *et al.*, 2005; Kokfelt *et al.*, 2006; Peate *et al.*, 2009, 2010). (c) K/Ti vs Zr/Y. Whole-rock compositions are shown with smaller symbols. The dotted fields enclose melt inclusion compositions from two Yemen flood basalt samples (Kent *et al.*, 2002). Symbols as in Fig. 4.

melting process not apparent from whole-rock analyses. The expected negative correlation between Zr content and the degree of silica saturation is better developed in the melt inclusions compared with the whole-rocks and Mull Plateau Group lavas as a whole (Fig. 11a; Kerr, 1995*b*), confirming that alteration modifies the whole-rock normative compositions.

Kent *et al.* (2002) showed that olivine-hosted melt inclusions with crustally contaminated compositions in Yemen flood basalts also had large variations in trace element ratios that can fractionate during melting in an upwelling mantle column, but are largely insensitive to crustal contamination (e.g. Zr/Y). They inferred that aggregation of melt from different parts of the upwelling mantle column took place within the crust, concurrent with crustal assimilation. Maclennan (2008) showed that the variability of incompatible trace element ratios in melt inclusions from Icelandic basalts decreases with decreasing forsterite content of the host olivine, as a result of concurrent melt aggregation and crystallization in lower crustal magma chambers. There are significant variations in Zr/Y in Mull Plateau Group lavas (e.g. Kerr, 1995*b*), but melt inclusions within single samples show a more limited range in Zr/Y values coupled with a wide range in K/Ti values (Fig. 11c). This potentially indicates that the melt aggregation process occurred earlier than the growth of the olivines found in the samples, with the caveat that the limited Zr/Y variability might reflect the small amount of inclusion data available for single Mull samples. Although K/Ti ratios can potentially be fractionated within the melting column, the lack of variability in Zr/Y confirms that K/Ti variations in the melt inclusions are dominated by crustal assimilation rather than melting processes.

SUMMARY

This study has demonstrated the potential of olivine-hosted melt inclusions to recover magmatic compositions of fluid-mobile elements (e.g. Na, K, Ba) in old, hydrothermally altered, lavas. Although the four studied Mull Plateau Group lavas have broadly similar whole-rock major element compositions that classify the samples as tholeiites, the melt inclusions span the range from more depleted tholeiite compositions to clearly alkaline magmas. Melt inclusions from single samples show systematic correlations between alkalis (K + Na) and incompatible element ratios such as Zr/Y, as expected for compositional variations related to different degrees of melting of a heterogeneous source. For the two incompatible-element-enriched alkaline samples, the melt inclusions have similar K/Ti to the whole-rocks, although the scatter in K/Ti of single inclusions can be explained by minor crustal assimilation during olivine crystallization. In contrast, melt inclusions in the two incompatible-element-depleted tholeiitic samples have less contaminated compositions than the whole-rocks, and also

show broad trends of increasing K/Ti (extent of assimilation) with decreasing Fo% of the host olivine (extent of differentiation) that indicate that crustal assimilation was concurrent with olivine growth. The overall compositional variations within the Mull Plateau Basalt group lavas indicate that the most primitive samples (>8 wt % MgO) show the greatest extents of crustal assimilation; the melt inclusion data from this study demonstrate that this occurred by an AFC process, in which assimilation is intimately linked to the crystallization of olivine.

ACKNOWLEDGEMENTS

Thanks go to Frank Tepley and Rick Hervig for assistance with the Oregon State EPMA and Arizona SIMS analyses respectively. John Maclennan, Leonid Danyushevsky and Greg Yaxley are thanked for their constructive reviews. The samples for this study were originally collected as part of the PhD project of Kevin Jones at Cardiff University (Jones, 2005). Sadly, Kevin died in 2009, and this paper is dedicated to his memory.

FUNDING

This work was supported by National Science Foundation grant EAR-0439888. The gas-mixing furnace laboratory at Iowa was established through funds from National Science Foundation grant EAR-0609652 and University of Iowa start-up funds to I.U.P. The ICP-MS facility at the University of Iowa was established through funding from the National Science Foundation (EAR-0821615) and the University of Iowa. The SIMS facility at Arizona State University is partly supported by a grant from the National Science Foundation.

SUPPLEMENTARY DATA

Supplementary data for this paper are available at *Journal of Petrology* online.

REFERENCES

Andreasen, R., Peate, D. W. & Brooks, C. K. (2004). Magma plumbing systems in large igneous provinces: inferences from cyclical variations in Palaeogene East Greenland basalts. *Contributions to Mineralogy and Petrology* **147**, 438–452.

Ariskin, A. A. (1999). Phase equilibria modeling in igneous petrology: use of COMAGMAT model for simulating fractionation of ferro-basaltic magmas and the genesis of high-alumina basalt. *Journal of Volcanology and Geothermal Research* **90**, 115–162.

Bailey, E. B., Clough, C. T., Wright, W. B., Richey, J. E. & Wilson, G. V. (1924). *Tertiary and post-Tertiary geology of Mull, Loch Aline and Oban. Memoirs of the Geological Survey of Great Britain.* London: HMSO.

Baker, J. A., Thirlwall, M. F. & Menzies, M. A. (1996). Sr–Nd–Pb isotopic and trace element evidence for crustal contamination of plume-derived flood basalts: Oligocene flood volcanism in western Yemen. *Geochimica et Cosmochimica Acta* **60**, 2559–2581.

Bamford, D., Nunn, K., Prodehl, C. & Jacob, B. (1977). LISP-III: upper crustal structure of northern Britain. *Journal of the Geological Society, London* **133**, 481–488.

Bohrson, W. A. & Spera, F. J. (2001). Energy-constrained open-system magmatic processes II: application of energy-constrained assimilation and fractional crystallization (EC-AFC) model to magmatic systems. *Journal of Petrology* **42**, 1019–1041.

Bohrson, W. A. & Spera, F. J. (2003). Energy-constrained open-system magmatic processes IV: geochemical, thermal and mass consequences of energy-contrained recharge, assimilation and fractional crystallization (EC-RAFC). *Geochemistry, Geophysics, Geosystems* **4(2)**, 8002, doi:10.1029/2002GC00316.

Bowen, N. L. (1928). *The Evolution of the Igneous Rocks*. Princeton, NJ: Princeton University Press, 334 p.

Brandon, A. D., Hooper, P. R., Goles, G. G. & Lambert, R. S. J. (1993). Evaluating crustal contamination in continental basalts: the isotopic composition of the Picture Gorge basalts of the Columbia River Basalt Group. *Contributions to Mineralogy and Petrology* **114**, 452–464.

Carmichael, I. S. E. (2004). Comments on Bailey *et al*. (1924). In: Carmichael, I. S. E. (ed.) *Landmark Papers: Volcanic Petrology.* Twickenham: Mineralogical Society of Great Britain & Northern Ireland, pp. L3–L4.

Chambers, L. M. & Fitton, J. G. (2000). Geochemical transitions in the ancestral Iceland plume: evidence from the Isle of Mull Tertiary volcano, Scotland. *Journal of the Geological Society, London* **157**, 261–264.

Chambers, L. M. & Pringle, M. S. (2001). Age and duration of activity at the Isle of Mull Tertiary igneous centre, Scotland, and confirmation of the existence of subchrons during Anomaly 26r. *Earth and Planetary Science Letters* **193**, 333–345.

Davidson, J. P., Morgan, D. J., Charlier, B. L. A., Harlou, R. & Hora, J. M. (2007). Microsampling and isotopic analysis of igneous rocks: implications for the study of magmatic systems. *Annual Review of Earth and Planetary Sciences* **35**, 273–311.

Danyushevsky, L. V., Della-Pasqua, F. N. & Sokolov, S. (2000). Re-equilibration of melt inclusions trapped by magnesian olivine phenocrysts from subduction-related magmas: petrological implications. *Contributions to Mineralogy and Petrology* **138**, 68–83.

Danyushevsky, L. V., Perfit, M. R., Eggins, S. M. & Falloon, T. J. (2003). Crustal origin for coupled 'ultra-depleted' and 'plagioclase' signatures in MORB olivine-hosted melt inclusions: evidence from the Siqueiros Transform Fault, East Pacific Rise. *Contributions to Mineralogy and Petrology* **144**, 619–637.

Danyushevsky, L. V., Leslie, R. A. J., Crawford, A. J. & Durance, P. (2004). Melt inclusions in primitive olivine phenocrysts: the role of localized reaction processes in the origin of anomalous compositions. *Journal of Petrology* **45**, 2531–2553.

DePaolo, D. J. (1981). Trace element and isotopic effects of combined wallrock assimilation and fractional crystallisation. *Earth and Planetary Science Letters* **53**, 189–202.

Dickin, A. P. (1981). Isotope geochemistry of Tertiary igneous rocks from the Isle of Skye, N.W. Scotland. *Journal of Petrology* **22**, 155–189.

Font, L., Davidson, J. P., Pearson, D. G., Nowell, G. M., Jerram, D. A. & Ottley, C. J. (2008). Sr and Pb isotope micro-analysis of plagioclase crystals from Skye lavas: an insight into open-system processes in a flood basalt province. *Journal of Petrology* **49**, 1449–1471.

Forester, R. W. & Taylor, H. P. (1976). ^{18}O-depleted igneous rocks from the Tertiary complex of the Isle of Mull, Scotland. *Earth and Planetary Science Letters* **32**, 11–17.

Fowler, S., Bohrson, W. A. & Spera, F. J. (2004). Magmatic evolution of the Skye Igneous Centre, Western Scotland: modelling of

assimilation, recharge and fractional crystallisation. *Journal of Petrology* **45**, 2481–2505.

Ghiorso, M. S. & Sack, R. O. (1995). Chemical mass transfer in magmatic processes. IV. A revised and internally consistent thermodynamic model for the interpolation and extrapolation of liquid–solid equilibria in magmatic systems at elevated temperatures and pressures. *Contributions to Mineralogy and Petrology* **119**, 197–212.

Halter, W. E., Pettke, T., Heinrich, C. A. & Rothern-Rutishauser, B. (2002). Major to trace element analysis of melt inclusions by laser ablation ICP-MS: methods of quantification. *Chemical Geology* **183**, 63–86.

Hawkesworth, C. J. & Morrison, M. A. (1978). A reduction in $^{87}Sr/^{86}Sr$ during basalt alteration. *Nature* **276**, 381–383.

Herzberg, C. & Asimow, P. D. (2008). Petrology of some oceanic island basalts: PRIMELT2.XLS software for primary magma calculation. *Geochemistry, Geophysics, Geosystems* **9**, Q09001, doi:10.1029/2008GC002057.

Humphris, S. E., Morrison, M. A. & Thompson, R. N. (1978). Influence of rock crystallisation history upon subsequent lanthanide mobility during hydrothermal alteration of basalts. *Chemical Geology* **23**, 125–137.

Huppert, H. E. & Sparks, R. S. J. (1985). Cooling and contamination of mafic and ultramafic magmas during ascent through continental crust. *Earth and Planetary Science Letters* **74**, 371–386.

Irvine, T. N. & Baragar, W. R. A. (1971). A guide to the chemical classification of the common igneous rocks. *Canadian Journal of Earth Sciences* **8**, 523–548.

Jones, K. (2005). The laser ablation ICP-MS analysis of olivine-hosted melt inclusions from the Mull Plateau Group lavas, Mull, Scotland, PhD thesis, Cardiff University, 278 p.

Kamenetsky, M. B., Sobolev, A. V., Kamenetsky, V. S., Maas, R., Danyushevsky, L. V., Thomas, R., Pokhilenko, N. P. & Sobolev, N. V. (2004). Kimberlitic melts rich in alkali chlorides and carbonates: a potent metasomatic agent in the mantle. *Geology* **32**, 845–848.

Kent, A. J. R (2008). Melt inclusions in basaltic and related volcanic rocks. In: Putirka, K. D. & Tepley, F. J., III (eds) *Minerals, Inclusions and Volcanic Processes. Mineralogical Society of America and Geochemical Society, Reviews in Mineralogy and Geochemistry* **69**, 273–331.

Kent, A. J. R., Baker, J. A. & Wiedenbeck, M. (2002). Contamination and melt aggregation processes in continental flood basalts: constraints from melt inclusions in Oligocene basalts from Yemen. *Earth and Planetary Science Letters* **202**, 577–594.

Kerr, A. C. (1995*a*). The geochemical stratigraphy, field relations and temporal variation of the Mull–Morvern Tertiary lava succession, NW Scotland. *Transactions of the Royal Society of Edinburgh: Earth Sciences* **86**, 35–47.

Kerr, A. C. (1995*b*). The geochemistry of the Mull–Morvern Tertiary lava succession, NW Scotland: an assessment of mantle sources during plume-related volcanism. *Chemical Geology* **122**, 43–58.

Kerr, A. C. (1998). Mineral chemistry of the Mull–Morvern Tertiary lava succession, western Scotland. *Mineralogical Magazine* **62**, 295–312.

Kerr, A. C., Kempton, P. D. & Thompson, R. N. (1995). Crustal assimilation during turbulent ascent (ATA): new isotopic evidence from the Mull Tertiary lava succession, N.W. Scotland. *Contributions to Mineralogy and Petrology* **119**, 142–154.

Kerr, A. C., Kent, R. W., Thomson, B. A., Seedhouse, J. K. & Donaldson, C. H. (1999). Geochemical evolution of the Tertiary Mull volcano, western Scotland. *Journal of Petrology* **40**, 873–908.

Klein, E. M. & Langmuir, C. H. (1987). Global correlations of ocean ridge basalt chemistry with axial depth and crustal thickness. *Journal of Geophysical Research* **94**, 4241–4252.

Kokfelt, T. F., Hoernle, K., Hauff, F., Fiebig, J., Werner, R. & Garbe-Schönberg, D. (2006). Combined trace element and Pb–Nd–Sr–O isotope evidence for recycled oceanic crust (upper and lower) in the Iceland mantle plume. *Journal of Petrology* **47**, 1705–1749.

Larsen, L. M. & Pedersen, A. K. (2000). Processes in high-Mg, high-T magmas: evidence from olivine, chromite and glass in Palaeogene picrites from West Greenland. *Journal of Petrology* **41**, 1071–1098.

Le Bas, M. J., Le Maitre, R. W., Streckeisen, A. & Zanettin, B. (1986). A chemical classification of volcanic rocks based on total alkali–silica diagram. *Journal of Petrology* **27**, 745–750.

Macdonald, G. A. & Katsura, T. (1964). Chemical composition of Hawaiian lavas. *Journal of Petrology* **5**, 82–133.

Maclennan, J. (2008). Concurrent mixing and cooling of melts under Iceland. *Journal of Petrology* **49**, 1931–1953.

McDonough, W. F. & Ireland, T. R. (1993). Intraplate origin of komatiites inferred from trace elements in glass inclusions. *Nature* **365**, 432–434.

Middlemost, E. A. K. (1975). The basalt clan. *Earth-Science Reviews* **11**, 337–364.

Morrison, M. A. (1978). Use of immobile trace elements to distinguish paleotectonic affinities of metabasalts—applications to Paleocene basalts of Mull and Skye, northwest Scotland. *Earth and Planetary Science Letters* **39**, 407–416.

Nielsen, R. L., Michael, P. J. & Sours-Page, R. (1998). Chemical and physical indicators of compromised melt inclusions. *Geochimica et Cosmochimica Acta* **62**, 831–839.

Peate, D. W. & Hawkesworth, C. J. (1996). Lithospheric to asthenospheric transition in low-Ti flood basalts from southern Paraná, Brazil. *Chemical Geology* **127**, 1–24.

Peate, D.W., Baker, J. A., Blichert-Toft, J., Hilton, D., Storey, M., Kent, A. J. R., Brooks, C. K., Hansen, H., Pedersen, A. K. & Duncan, R. A. (2003). The Prinsen af Wales Bjerge Formation lavas, East Greenland: the transition from tholeiitic to alkalic magmatism during Palaeogene continental break-up. *Journal of Petrology* **44**, 279–304.

Peate, D. W., Barker, A. K., Riishuus, M. S. & Andreasen, R. (2008). Temporal variations in crustal assimilation of magma suites in the East Greenland flood basalt province: tracking the evolution of magmatic plumbing systems. *Lithos* **102**, 179–197.

Peate, D. W., Baker, J. A., Jakobsson, S. P., Waight, T. E., Kent, A. J. R., Grassineau, N. & Skovgaard, A. C. (2009). Historic magmatism on the Reykjanes Peninsula, Iceland: a snap-shot of melt generation at a ridge segment. *Contributions to Mineralogy and Petrology* **157**, 359–382.

Peate, D. W., Breddam, K., Baker, J. A., Kurz, M., Barker, A. K., Prestvik, T., Grassineau, N. & Skovgaard, A. C. (2010). Compositional characteristics and spatial distribution of enriched Icelandic mantle components. *Journal of Petrology* **51**, 1447–1475.

Preston, R. J., Bell, B. R. & Rogers, G. (1998). The Loch Scridain xenolithic sill complex, Isle of Mull, Scotland: fractional crystallization, assimilation, magma-mixing and crustal anatexis in subvolcanic conduits. *Journal of Petrology* **39**, 519–550.

Roedder, E. & Emslie, R. (1970). Olivine–liquid equilibrium. *Contributions to Mineralogy and Petrology* **29**, 275–289.

Rowe, M. C., Nielsen, R. L. & Kent, A. J. R. (2006). Anomalously high Fe contents in rehomogenized olivine hosted melt inclusions from oxidized magmas. *American Mineralogist* **91**, 82–91.

Rowe, M. C., Kent, A. J. R. & Nielsen, R. L. (2007). Determination of sulfur speciation and oxidation state of olivine hosted melt inclusions. *Chemical Geology* **236**, 303–322.

Rowe, M. C., Peate, D. W. & Newbrough, A. (2011). Compositional and thermal evolution of olivine-hosted melt inclusions in small-volume basaltic eruptions: a 'simple' example from Dotsero

volcano, NW Colorado. *Contributions to Mineralogy and Petrology* **161**, 197–211.

Saunders, A. D., Fitton, J. G., Kerr, A. C., Norry, M. J. & Kent, R. W. (1997). The North Atlantic Igneous Province. In: Mahoney, J. J. & Coffin, M. F (eds) *Large Igneous Provinces: Continental, Oceanic and Planetary Flood Volcanism. American Geophysical Union, Geophysical Monograph* **100**, 45–93.

Scarrow, J. H. & Cox, K. G. (1995). Basalts generated by decompressive adiabatic melting of a mantle plume: a case study from the Isle of Skye, NW Scotland. *Journal of Petrology* **36**, 3–22.

Sinton, J., Grönvold, K. & Saemundsson, K. (2005). Postglacial eruptive history of the Western Volcanic Zone, Iceland. *Geochemistry, Geophysics, Geosystems* **6(12)**, Q12009, doi:10.1029/2005GC001021.

Sobolev, A. V., Hofmann, A. W., Kuzmin, D. V., Yaxley, G. M., Arndt, N. T., Chung, S.-L., Danyushevsky, L. V., Elliott, T., Frey, F. A., Garcia, M. O., Gurenko, A. A., Kamenetsky, V. S., Kerr, A. C., Krivolutskaya, N. A., Matvienkov, V. V., Nikogosian, I. K., Rocholl, A., Sigurdsson, I. A., Sushchevskaya, N. M. & Teklay, M. (2007). The amount of recycled crust in sources of mantle-derived melts. *Science* **316**, 412–417.

Sun, S. S. & McDonough, W. F. (1989). Chemical and isotopic systematics of oceanic basalts: implications for mantle composition and processes. In: Saunders, A. D. & Norry, M. J. (eds) *Magmatism in the Ocean Basins. Geological Society, London, Special Publications* **42**, 313–347.

Tanaka, T., Togashi, S., Kamioka, H., Amakawa, H., Kagami, H., Hamamoto, T., Yuhara, M., Orihashi, Y., Yoneda, S., Shimizu, H., Kunimaru, T., Takahashi, K., Yanagi, T., Nakano, T., Fujimaki, H., Shinjo, R., Asahara, Y., Tanimizu, M. & Dragusanu, C. (2000). JNdi-1: a neodymium isotopic reference in consistency with LaJolla neodymium. *Chemical Geology* **168**, 279–281.

Thompson, R. N., Dickin, A. P., Gibson, I. L. & Morrison, M. A. (1982). Elemental fingerprints of isotopic contamination of Hebridean Palaeocene mantle-derived magmas by Archaean sial. *Contributions to Mineralogy and Petrology* **79**, 159–168.

Tilley, C. E. & Muir, I. D. (1962). The Hebridean Plateau magma type. *Transactions of the Edinburgh Geological Society* **19**, 208–215.

Walker, G. P. L. (1970). The distribution of amygdale minerals in Mull and Morvern (Western Scotland). In: Murty, T. V. V. G. G. R. K. & Rao, S. S. (eds) *W. D. West Commemorative Volume, University of Saugar, India. Studies in Earth Sciences*, pp. 181–194.

Whitehouse, M. J. (1990). Isotopic evolution of the southern Outer Hebridean Lewisian gneiss complex: constraints on Late Archaean source regions and the generation of transposed Pb–Pb palaeoisochrons. *Chemical Geology* **86**, 1–20.

Whitehouse, M. J. & Robertson, C. J. (1995). Isotopic evolution of the Lewisian Complex of Tiree, Inner Hebrides and correlation with the mainland. *Scottish Journal of Geology* **31**, 131–137.

Yaxley, G. M., Kamenetsky, V. S., Kamenetsky, M., Norman, M. D. & Francis, D. (2004). Origins of compositional heterogeneity in olivine-hosted melt inclusions from the Baffin Island picrites. *Contributions to Mineralogy and Petrology* **148**, 426–442.